

LABORATORI NAZIONALI DI FRASCATI

SIS – Pubblicazioni

LNF-98/023 (P)

27 Luglio 1998

DAΦNE Machine Project

Contributions to the
Sixth European Particle Accelerator Conference (EPAC 98)
Stockholm, 22 to 26 June 1998

CONTENTS

Invited

DAΦNE Commissioning

C. Biscari and DAΦNE Commissioning Team	1
---	---

Contributed

DAΦNE Linac Operational Performances

R. Boni, F. Marcellini, F. Sannibale, M. Vescovi, G. Vignola	6
--	---

Performance and Operation of the DAΦNE Accumulator

M.E. Biagini, C. Biscari, R. Boni, V. Chimenti, A. Clozza, S. De Simone, G. Di Pirro, A. Drago, A. Gallo, A. Ghigo, S. Guiducci, F. Marcellini, M.R. Masullo, C. Milardi, L. Pellegrino, M.A. Preger, C. Sanelli, F. Sannibale, M. Serio, F. Sgamma, B. Spataro, A. Stecchi, A. Stella, G. Vignola, M. Zobov	9
---	---

DAΦNE Main Rings Optics

M. Bassetti, M.E. Biagini, C. Biscari, S. Guiducci, M.R. Masullo, C. Milardi, M.A. Preger, G. Vignola	12
--	----

DAΦNE Control System Status and Performance

G. Di Pirro, A. Drago, G. Mazzitelli, C. Milardi, F. Sannibale, A. Stecchi, A. Stella	15
---	----

Implementation and Performance of the DAΦNE Timing System

G. Di Pirro, A. Drago, A. Gallo, A. Ghigo, F. Sannibale, M. Serio	18
---	----

DAΦNE Magnet Power Supply Systems

R. Ricci, C. Sanelli, A. Stecchi	21
--	----

Installation and alignment of the DAΦNE Accelerators

C. Biscari, F. Sgamma	24
-----------------------------	----

The DAΦNE Cooling System

L. Pellegrino	27
---------------------	----

DAΦNE COMMISSIONING

C. Biscari, DAΦNE Commissioning Team*, LNF-INFN, Frascati, Italy

Abstract

We report the main results of DAΦNE commissioning, which is underway and is expected to be completed by next autumn, when the KLOE detector will be rolled in to begin physics run.

1 INTRODUCTION

The construction and installation phase of DAΦNE [1], the Frascati Φ-factory, have been completed in autumn 1997 (see Fig. 1).

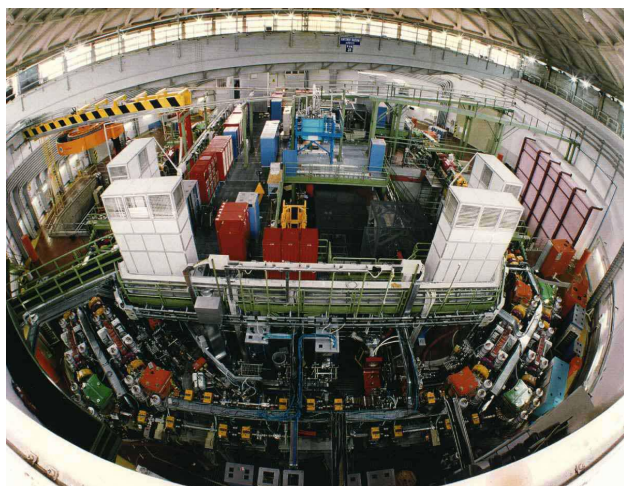


Figure 1: DAΦNE hall (June 1998)

The approach of DAΦNE to high luminosity, multi-bunch flat beams with a very high current stored in two separate rings, is common to the other two factories presently under construction, KEK-B [2] and PEP-II [3].

The electron and positron beams collide in two Interaction Points (IP). The crossing at a horizontal angle of 25 mrad minimizes the effect of parasitic collisions and it allows to store up to 120 bunches per ring, corresponding to a colliding frequency of 368.26 MHz. The high rate of bunch collisions relaxes the single bunch luminosity parameters.

The magnetic layout of DAΦNE is shown in Fig. 2, while the main design parameters are reported in Table 1.

* M. Bassetti, M.E. Biagini, R. Boni, V. Chimenti, A. Clozza, G. Delle Monache, S. De Simone, G. Di Pirro, A. Drago, A. Gallo, A. Ghigo, S. Guiducci, F. Marcellini, M.R. Masullo, G. Mazzitelli, C. Milardi, L. Pellegrino, M.A. Preger, R. Ricci, C. Sanelli, F. Sannibale, M. Serio, F. Sgamma, B. Spataro, A. Stecchi, A. Stella, C. Vaccarezza, M. Vescovi, G. Vignola, M. Zobov.

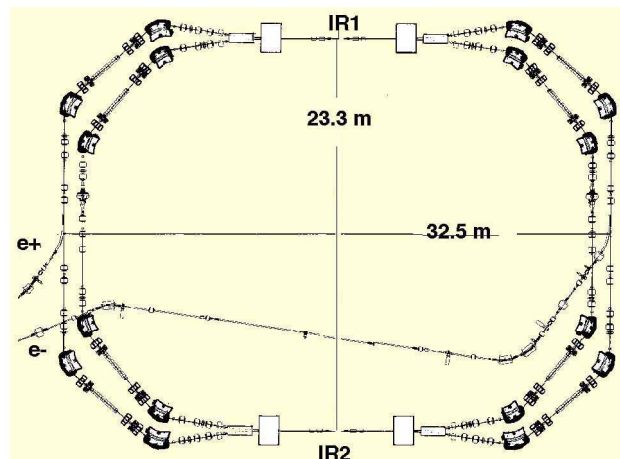


Figure 2: DAΦNE magnetic layout

Table 1: DAΦNE Design Parameters

Energy [GeV]	0.51
Maximum luminosity [$\text{cm}^{-2}\text{s}^{-1}$]	5.3×10^{32}
Single bunch luminosity [$\text{cm}^{-2}\text{s}^{-1}$]	4.4×10^{30}
Trajectory length (each ring) [m]	97.69
Emittance, ϵ_x/ϵ_y [mm·mrad]	1/0.01
Beta function, $\beta^{*,x}/\beta^{*,y}$ [m]	4.5/0.045
Transverse size $\sigma^{*,x}/\sigma^{*,y}$ [mm]	2/0.02
Beam-beam tune shift, ξ_x/ξ_y	0.04/0.04
Crossing angle, θ_x [mrad]	25
Betatron tune, ν_x/ν_y	5.09/5.07
RF frequency, f_{RF} [MHz]	368.26
Number of bunches	120
Minimum bunch separation [cm]	81.4
Particles/bunch [10^{10}]	8.9
RF voltage [MV]	0.250
Bunch length σ_L [cm]	3.0
Synchrotron radiation loss [keV/turn]	9.3
Damping time, τ_e/τ_x [ms]	17.8/36.0

The collider commissioning without experiments (*day-one* configuration) is well advanced. The roll in of KLOE [4] detector on the first IP is scheduled by next fall and starts of physics run by the end of the year. FINUDA [5] roll-in will come later and in the meantime the DEAR [6] experiment will take data on the second IP.

The injector system, consisting of a full energy LINAC and a damping ring (Accumulator), is described in detail in this conference [7, 8].

The injector commissioning has been carried out in parallel with the main rings installation, for a total period of two months spread along two years. The LINAC and Accumulator performance have exceeded the design values and both operate in a reliable way.

2 MAIN RING OVERVIEW

Electrons and positrons are stored in two symmetric rings, intersecting in two points and sharing two Interaction Regions (IR), where beams travel in the same vacuum chamber, passing off-axis in the low beta quadrupoles. At the end of each IR the beams are separated by 12 cm and a splitter magnet, with two independent vacuum chambers, drives the two beams in the corresponding rings.

The ring periodic structure consists of four arcs. The straight sections orthogonal to the IRs are used for injection, RF and feedback kickers. The arc cell, named BWB (Bending-Wiggler-Bending) [9], is quasi-achromatic, its special feature being the presence of a 1.8 T wiggler, 2 m long, in the region of maximum dispersion, which doubles up the synchrotron radiation emitted in the dipoles. The damping times are shortened and instabilities thresholds are raised. The wiggler allows also emittance tuning at constant field by appropriate control of the dispersion function. Moreover, the resulting increase of the natural energy fluctuation should raise the beam-beam tune shift limit [10].

To make optics flexible all quadrupoles and sextupoles are independently powered. There are 480 power supplies [11], ranging from 100 VA to 1500 kVA. The very different output currents ($10\div 2300$ A) and output voltages ($8\div 1300$ V) have led to different technical solution realized by various industries (Danfysik - Denmark, Hazemeyer - France, Inverpower - Canada, OCEM - Italy).

Special RF cavities, with low impedances parasitic high order modes (HOM) content, have been developed [12] to allow stable high current-multibunch operation. The cavities, one per ring, are normal conducting copper single cells, with a system of HOM damping waveguides which couple out and dissipate the HOM energy induced by the beam on external $50\ \Omega$ loads. The HOM shunt impedances have been reduced by orders of magnitude. The operation of the damped cavities has been until now very successful, without any evidence of arcing or multipacting effects due to the loading waveguides.

A longitudinal bunch-by-bunch feedback system [13] has been implemented in collaboration with the SLAC/LBL PEP II group to damp beam residual oscillations. It consists of a scalable time domain system employing digital techniques. A wideband kicker cavity has been developed at LNF [14].

A timing system [15] provides the synchronization of the Main Ring (MR) RF cavities, the Accumulator RF

phase, the firing instant of the Linac, the injection/extraction kickers in the accumulator ring and the MR injection kickers in order to fill the selected bucket, with a precision down to a few picoseconds.

The Control System [16] is completely based on personal computers. The commercial software LabVIEW has been chosen at any level and the hardware interface is based on specially developed MacIntosh boards in a VME environment. The machine devices are driven by several distributed CPUs. A shared memory instead of a network permits fast, easy, and high bandwidth communications. The Control System has allowed the step by step commissioning of the major DAΦNE subsystems as they were installed, proving to be modular and extensible.

3 SINGLE RING COMMISSIONING

The initial commissioning phase of the collider has been dedicated to optimize the single bunch luminosity. Single ring commissioning has therefore been focused on full characterization and equalization of the single bunch luminosity parameters of both rings. The start up has been done directly on design IP parameters, i.e., nominal betatron functions (β^*) at the IP and nominal crossing angle.

Being DAΦNE a low energy machine the IR optics is highly influenced by the experimental detector solenoidal fields. The KLOE detector, for example, (0.6 T x 4 m magnetic field) will introduce focusing effects plus a rotation of $\sim 45^\circ$ in the transverse plane which will be cancelled by external compensating solenoids.

For the collider commissioning in the absence of experiments, two *day-one* IRs with conventional quadrupoles and no solenoids, have been installed in the experimental pits. From the optics point of view the IR first order matrix is equal to the IR experimental matrix, while the chromatic contribution is weaker, since quadrupole arrangements had no space constraints. Figure 3 shows the IR betatron functions.

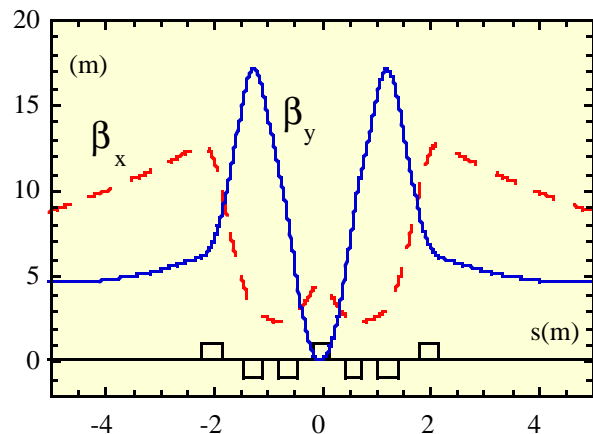


Figure 3: *Day-one* IR betatron functions

The closed orbit has been corrected in both rings to rms values of 1 ~ 2 mm.

Since the two rings are close to each other (see Figs. 1, 2) the magnetic cross-talk is not negligible, as was already estimated from magnetic measurements. Fringing fields of dipoles, wigglers, splitters and elements of the transfer lines produce orbit and tune shifts on the near ring mainly in the horizontal plane. Measurement and correction of these effects have been successfully carried out. The horizontal closed orbit is also influenced by the compensation of the trajectory in the wigglers ($\int B dl = 0$ on the trajectory), by the splitter magnet set point as a function of the crossing angle at the IP and by the balance between the splitter and the dipole field. The vertical closed orbit with no correction is stable in both machines: this is a cross-check of the goodness of the alignment [17].

The Beam Position Monitor (BPM) system includes striplines for single pass measurements and button monitors for accurate measurements on the stored beam. The electronics for the BPM detectors has been developed by BERGOZ Beam Instrumentation System. An example of the corrected orbit on the electron ring is given in Fig. 4.

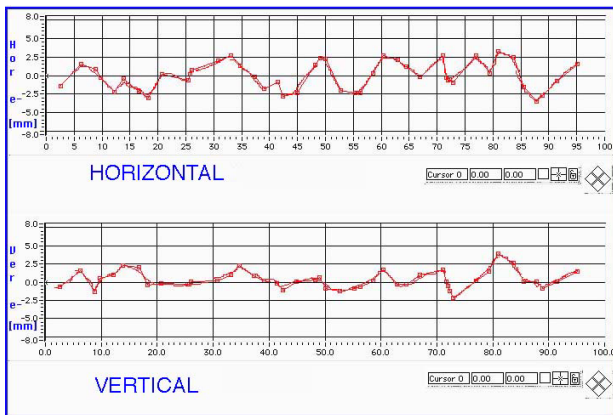


Figure 4: Corrected closed orbit in e^- ring

Extensive measurements of optical functions and chromaticity have been done. A quite satisfactory agreement has been reached between measurements and a machine modeling which includes fringing effects of wigglers, small curvature radius dipoles, quadrupoles and off-axis effects of low-beta quadrupoles. No evidence of dynamic aperture limits has been found.

Coupling has been measured and corrected by powering few of the installed skew quadrupoles. The bunch dimensions were measured with the synchrotron light monitors. Since the vertical resolution was not sufficient, beam lifetime measurements have been used to minimize the coupling: in fact the beam lifetime τ is Touschek dominated, and for a given bunch current, minimum coupling corresponds to maximum bunch density and to minimum τ . The estimated coupling is around the nominal 1% for the positron beam, which is again a check of the good magnet alignment. In the e^- ring the ratio of the vertical emittance

to the horizontal one is also $\sim 1\%$ at low current; as the current increases the emittance blow-up due to ion trapping leads to vertical dimension increase.

Special care has been put on the minimisation of the coupling impedance. The contribution of every vacuum system element to the impedance budget has been accurately assessed.

The bunch length as a function of the bunch current has been measured in the positron ring. Figure 5 shows a comparison of the measured bunch length with the results of numerical simulations which were carried out much before the measurements [18]. The agreement is really satisfactory. The normalised longitudinal coupling impedance $|Z/n|$ estimated from both the measurement and the simulation results is equal to 0.6Ω .

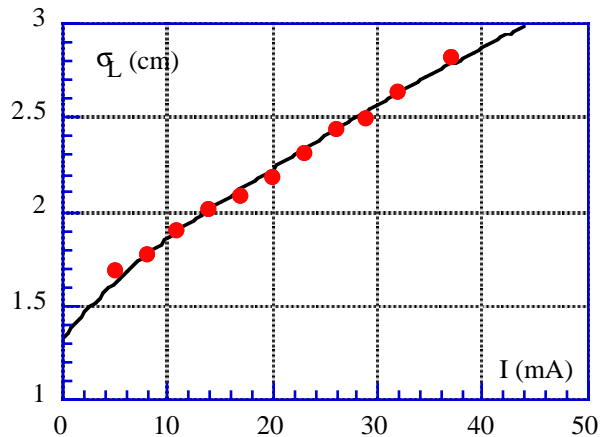


Figure 5: Bunch length simulations (solid line) and measurements (dots) in the e^+ ring

Most components of the vacuum chamber have been baked out before the installation. No bake-out has been done in-situ so far. The vacuum has been improved by beam-conditioning: several night shifts have been dedicated to clean the vacuum walls by waving vertically the beam at the maximum available current. Titanium sublimation pumps have been activated few times. The present static average pressure in the rings is ≤ 1 nanotorr. The pressure rise due to the beam is still high and evidence of ion trapping in the electron ring has been found even in the single bunch mode. Tune spread and shift have been measured. The ion clearing system has been preliminarily tested, partially powered, with several bunch filling configurations. No evidence of photo-electron instabilities in the positron ring has been so far detected.

The nominal single bunch current of 44 mA has been exceeded in both positron and electron rings: 90 mA of positrons and 110 mA of electrons have been stored with no active feedback and with no evidence of harmful instabilities. In particular, the transverse mode coupling threshold has not been reached.

The threshold of head-tail instability with no sextupoles is of the order of 10 mA in both rings with the present chromaticities.

A few hundreds of mA have been stored in both rings with different multibunch configurations.

In spite of no dedicated machine time spent in studying and optimising multibunch injection and operation, the longitudinal bunch by bunch feedback systems have been set-up [13] and are operational in both rings. In particular, damping times in the millisecond region are routinely obtained and consistently measured. A damping time faster than $\sim 200 \mu\text{sec}$ has been demonstrated in the positron ring with 30 bunches. Figure 6 shows the beam spectrum with feedback off and on in the positron ring.

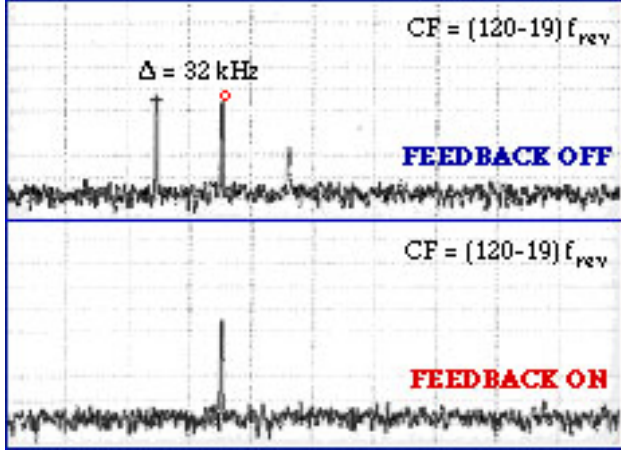


Figure 6: Beam spectrum without and with feedback in the positron ring, 30 bunches, 70 mA

4 SINGLE BUNCH LUMINOSITY

The design value of the beam-beam tune shift is 0.04. The design betatron working point has been chosen on the basis of beam-beam simulations [19] which include crossing angle, finite bunch length, variation of β along the bunch during collisions and energy loss due to longitudinal effects. The optimum operating point is of course near the integer.

Since in the first runs of single ring operation the rings were tuned on working points far from the integer, we have decided to make the first collisions in the tune zone already explored. According to simulations the chosen working point in this tune region is (5.15, 5.21) which provides a reasonable beam-beam tune shift parameters of $\xi = 0.02$. The corresponding current is 20 mA per bunch. Tail growth and beam blow up at larger currents are predicted.

The two rings have been separately tuned on the collision configuration, checking the symmetry of the two distinct β_y ; the two beam trajectories in the IR were aligned (see Fig. 7), especially benefiting of one BPM at the IP installed in the *day-one* vacuum chamber.

The longitudinal overlap of collisions at the nominal IP has been timed by monitoring the distance between the combined signals left on two sets of symmetric BPMs

around the IP by the incoming beam toward the IP and the outgoing one.

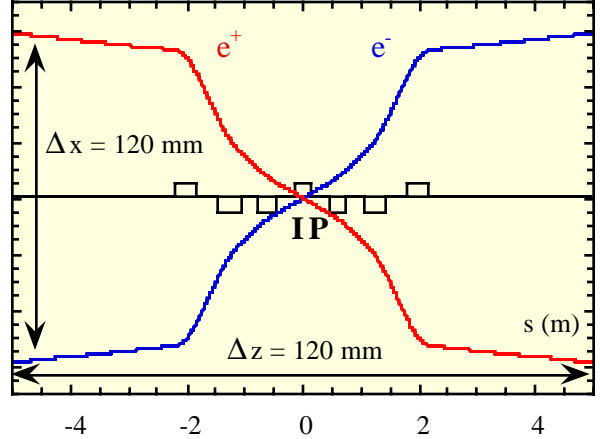


Figure 7: Beam trajectories in the IR.

The collisions have been done on one IP with the beams kept vertically separated at the other one.

A luminosity monitor [20] based on the measurement of the photons from the single bremsstrahlung (SB) reaction is used. The SB high counting rate allows fast monitoring, which is very useful during machine tune-up. The contribution of the gas bremsstrahlung reaction is subtracted by measuring the counting rate with two non interacting bunches. The estimated error on the measurements is of the order of 20%.

The luminosity has been also evaluated from beam-beam tune shift measurements and results are in good agreement with the luminosity monitor ones.

Sets of luminosity measurements have been executed during two different shifts. The results are summarized in Fig. 8. All the measurements correspond to good beam-lifetime in both beams and stable conditions. First runs dedicated to luminosity parameter tuning were done with bunch currents limited to few mA.

The design luminosity is $4.4 \cdot 10^{30} \text{ cm}^{-2} \text{ sec}^{-1}$ with 44 mA per bunch. Scaling it by the two beam currents, the design geometrical luminosity for nominal emittance, coupling and β^* is $2.2 \cdot 10^{27} \text{ cm}^{-2} \text{ sec}^{-1} \text{ mA}^{-2}$.

The maximum measured luminosity so far is:

$$4 \cdot 10^{29} \text{ cm}^{-2} \text{ sec}^{-1}.$$

Values of 60% the design geometrical luminosity have been consistently obtained. The maximum current per beam was about 20 mA, well in agreement with the $\xi = 0.02$ beam-beam simulations. Larger currents showed as expected emittance blow-up in the weaker beam and poor lifetime. Considering that the e^- emittance is enhanced by ion trapping, we can conclude that the basic single bunch luminosity parameters are in agreement with the design ones.

Next shifts will be done at the design working point for luminosity optimisation.

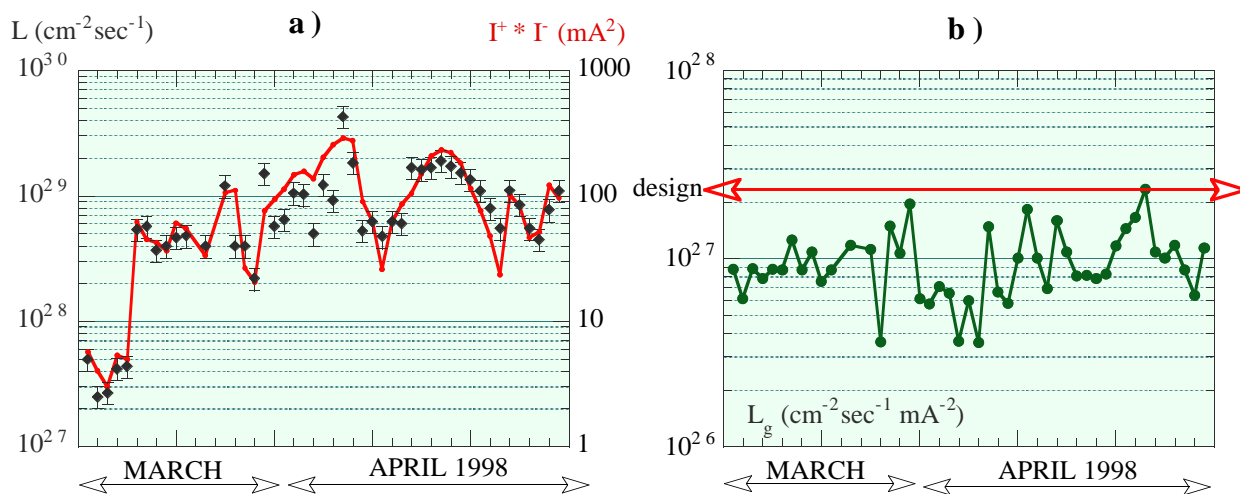


Figure 8: a) Luminosity (circles with error bars) and product of bunch currents (solid line); b) Geometrical luminosity

5 CONCLUSIONS

The results so far obtained during the first period of DAΦNE commissioning are in agreement with all the design parameters and there is no evidence of new accelerator physics.

The DAΦNE commissioning will continue to achieve the design luminosity, together with high current and multibunch operation optimization.

The commissioning with the KLOE detector, coinciding with the first physics data taking, is foreseen for the end of 1998.

6 ACKNOWLEDGMENTS

All the DAΦNE staff is indebted to the DAΦNE Machine Advisory Committee for the advice and support during the project and construction phase.

The authors thank all the DAΦNE technical staff for their enthusiasm and high level professionalism which has allowed to reach with success in a short time reliable operation.

Finally special thanks to Pina Possanza for her enthusiastic help in editing this paper.

REFERENCES

[1] G.Vignola and DAΦNE Project Team, DAΦNE: The First Φ-Factory, EPAC'96, Sitges, June 1996, p. 22.
 [2] S. Kurokawa, Present Status of KEK-B Project, these Proceedings.
 [3] J. Dorfan et al, PEP-II Status Report, these Proceedings
 [4] The KLOE collaboration, KLOE, a General Purpose Detector for DAΦNE, Frascati Internal Note LNF-92/109, April 1992.
 [5] The FINUDA collaboration, FINUDA, a detector for nuclear physics at DAΦNE, Frascati Internal Note LNF-93/021, May 1993.
 [6] The DEAR collaboration, The DEAR Proposal, LNF-95/055(IR), Oct.1995.

[7] R. Boni, F. Marcellini, F. Sannibale, M. Vescovi, G.Vignola, DAΦNE Linac Operational Performances, these Proceedings.
 [8] M.E. Biagini et al., Performance and Operation of the DAΦNE Accumulator, these Proceedings.
 [9] M. Bassetti, M.E. Biagini, C. Biscari, S. Guiducci, M.R. Masullo, C. Milardi, M.A. Preger, G.Vignola, DAΦNE Main Ring Optics, these Proceedings.
 [10] M. Bassetti, G. Vignola, Proposal for a Φ-Factory, LNF-90/031 (R), 1990.
 [11] R. Ricci, C. Sanelli, A. Stecchi, DAΦNE Magnet Power Supply System, these Proceeding.
 [12] R. Boni et al., High Power Test of the Waveguide Loaded RF Cavity for the Frascati Φ-Factory Main Rings, EPAC'96, Sitges, June 1996, p. 1979.
 [13] J.D. Fox et al., Multi-Bunch Longitudinal Dynamics and Diagnostics via a Digital Feedback System at PEP-II, DAΦNE, ALS and SPEAR, these Proceedings.
 [14] R. Boni, A. Gallo, A. Ghigo, F. Marcellini, M. Serio, M. Zobov, A Waveguide Overloaded Cavity as Longitudinal Kicker for the DAΦNE Bunch by Bunch Feedback System, Particle Accelerators, Vol. 52, pp. 95-113, 1996.
 [15] G. Di Pirro, A. Drago, A. Ghigo, F. Sannibale, M. Serio, Implementation and Performance of the DAΦNE Timing System, these Proceedings.
 [16] G. Di Pirro, G. Mazzitelli, C. Milardi, A. Stecchi, The DAΦNE Control System Status and Performance, these Proceedings.
 [17] C. Biscari, F. Sgamma, Installation and Alignment of the DAΦNE Accelerators, these Proceedings.
 [18] M. Zobov et. al., Collective Effects and Impedance Study for the DAΦNE Φ - Factory, Review Talk given at the International Workshop on Collective Effects and Impedance for B- Factories, Tsukuba, Japan, 12-17 June 1995. LNF-95/041(P), 31 July 1995. Also KEK Proceedings 96-6, August 1996 (A), pp. 110 - 155.
 [19] K. Hirata, M. Zobov, Beam-Beam Interaction Study for DAΦNE, EPAC'96, Sitges, June 1996, p.1158.
 [20] G. Di Pirro, A. Drago, A. Ghigo, G. Mazzitelli, M. Serio, F. Sannibale, G. Vignola, F. Cervelli, and T. Lomtadze, The DAΦNE Luminosity Monitor, 8th Beam Instrumentation Workshop, May 4-7, 1998, SLAC, Palo Alto, CA, USA.

DAΦNE LINAC OPERATIONAL PERFORMANCE

R. Boni, F. Marcellini, F. Sannibale, M. Vescovi, G. Vignola
LNF-INFN, Frascati, Italy

Abstract

DAΦNE, the Frascati Φ-Factory presently under commissioning, is an e^+/e^- collider whose injection system is composed by a ≈ 60 m Linac and by a ≈ 33 m long damping ring connected to each other and to the DAΦNE main rings by ≈ 180 m of transfer line. Both the positron and the electron beams are alternately produced and accelerated by the Linac up to the operation energy of 510 MeV. Because of the high peak and integrated luminosity requested to DAΦNE, the requirements concerning some of the relevant Linac features, in particular the value of the positron macrobunch peak current are very demanding. During the Linac operation all the design values have been achieved and in most cases surpassed. A description of the relevant operational performances of the DAΦNE Linac is presented.

1 INTRODUCTION

The first part of the Frascati Φ-Factory [1] injector is an S band (2856 MHz) Linac that alternately produces and accelerates the electron and positron beams up to the collider operation energy of 510 MeV. Before injection into the Main Rings the beams are stored into the Accumulator ring [2] for phase space damping. The Linac has been designed built and installed by the USA firm TITAN BETA [3], the system check-out has been done by TITAN and LNF personnel jointly, while the commissioning of both beams has been entirely performed by the LNF staff. The commissioning phase started on April 1996 and was concluded on February 1997. Since then the Linac has been operating on a base of 15 days per month.

Table 1: DAΦNE Linac beam parameters.

	Electron Mode		Positron Mode	
	Design	Achieved	Design	Achieved
Operation Energy (MeV)	510	510	510	510
rms Energy Spread (%)	0.5	0.56	1.0	0.95
Macrobunch Current (mA)	150	300	36	70
Macrobunch Length (ns)	10	10	10	10
Emittance @ 510 MeV (mm mrad)	1.0	< 10	10.0	< 10
Repetition Rate (pps)	50	50	50	50

Table 1 lists the Linac beam relevant parameters. The values on the table must be analyzed keeping in mind that the operation energy of the collider is fixed at 510 MeV and that the acceptance of the downstream transfer line and Accumulator ring is 1.5 % for the rms energy spread and 10 mm mrad for the emittance at 510 MeV. The high positron current obtained allows to significantly reduce the main rings injection time, with beneficial effects on the integrated luminosity in DAΦNE.

2 SYSTEM DESCRIPTION

In what follows a general description is presented, detailed information can be found in reference [4]. Figure 1 shows the RF Linac layout. In the positron mode about 5.5 A of electrons are accelerated up to ~ 200 MeV at the positron converter (PC) target for positron production and capture. An e^+/e^- separator kills the secondary electron beam produced during the conversion and allows the use of the downstream diagnostics for monitoring the positron beam only. In the electron mode the PC metallic target is extracted and the separator is turned off so that the electron beam can go directly to the Linac end.

The injector system includes a 150 keV max thermionic gun, a pre-buncher and a buncher both at 2856 MHz. All the 15 accelerating sections are the well known 2856 MHz 3 m long $2/3 \pi$ TW CG sections designed for the first time by SLAC. The necessary RF power is produced by 4 RF stations, each consisting of a 45 MW 4.5 μ sec klystron (Thomson TH2128C) and of a SLED pulse compressor. The accelerating gradient is about 17 MeV/m in all the sections and 24 MeV/m in the capture section (CS) where twice the RF power is applied. The energy gain due to the SLED is about 1.6. The positron converter scheme is based on the SLAC design: a removable tungsten-rhenium target is used for the pair production, while a flux concentrator jointly with DC solenoid magnets generate the 5 T peak magnetic field necessary for the positron capture. The focusing of the beam is obtained by a FODO arrangement of quadrupoles with pitch changing according to the beam energy. Solenoidal field magnets are used in the gun and PC areas. Beam Diagnostics include 14 beam position monitors, one at the end of each of the accelerating sections, 4 fluorescent screens placed at the end of E5 section, on the PC target, at the separator output and at the Linac end. Finally, 4 wall current monitors of the resistive type placed at the gun output, at the PC, at the separator output and at the Linac end, allow to measure the beam current along the Linac.

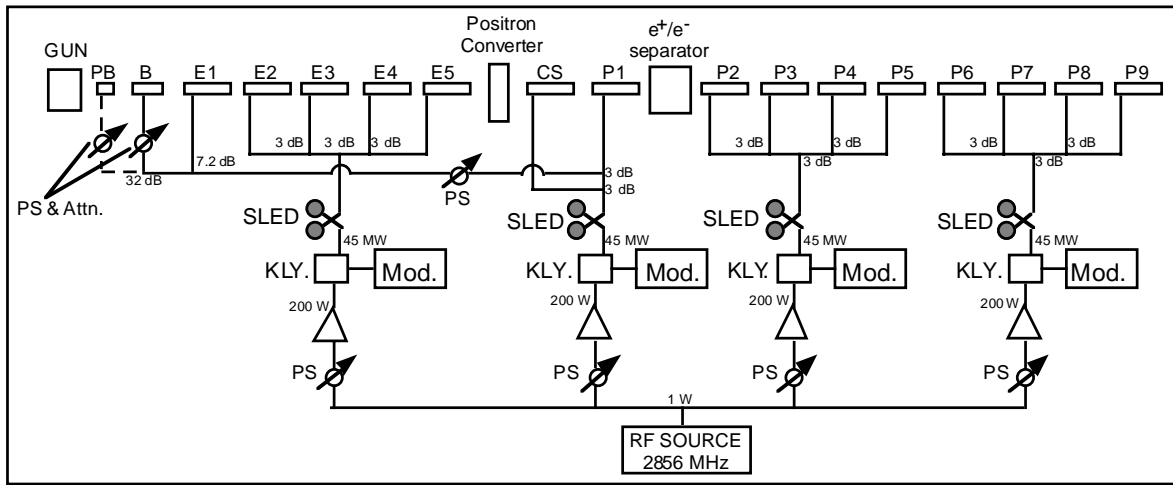


Figure 1: DAΦNE LINAC RF layout.

A CAMAC-Macintosh control system, with software in LabView, allows full remote control of the Linac. A separate GPIB controlled system based on two scopes and a wide band multiplexer is used for the system and beam diagnostics signals.

3 POSITRON MODE RESULTS

Figure 2 shows the signals from the 4 current monitors during a typical run in the positron operation mode. From left to right, the signals show 7.4 A (e^-), 5.7 A (e^-), 81 mA (e^+) and 67 mA (e^+) currents at the gun output, at the PC, at the separator output and at the Linac end respectively. The positron production efficiency, defined as the ratio between the positron current at the Linac output and the electron current at the positron converter, is 1.18 %.

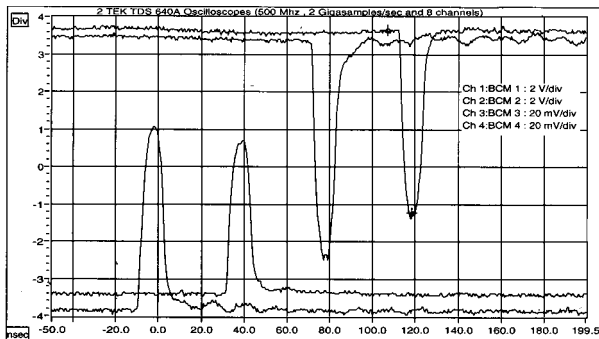


Figure 2: Current monitor signals in positron mode.

An estimate of the electron beam energy at the PC has been performed by using the corrector coil at the end of section E5 jointly with the profile monitor placed before the PC. The value obtained is ~ 190 MeV. The spot size at the PC target, measured by observing the thin fluorescent screen assembled in direct contact with the PC target surface, has a rms radius < 1 mm.

In Figure 3 the energy analyzer [5] control window shows a positron beam energy distribution at 510 MeV

with rms spread of 0.98 %. It is worth to point out (see figure 3) that 93% of the beam is within the energy acceptance of ± 1.5 % of the downstream transfer line and Accumulator ring.

Emittance measurements, not yet performed, are foreseen in the near future by using the 3 gradients method [6]. Anyway, simulations have shown that the overall acceptance of the Linac downstream the PC is < 10 mm mrad, so that this value can be assumed as a upper limit for the beam emittance value.

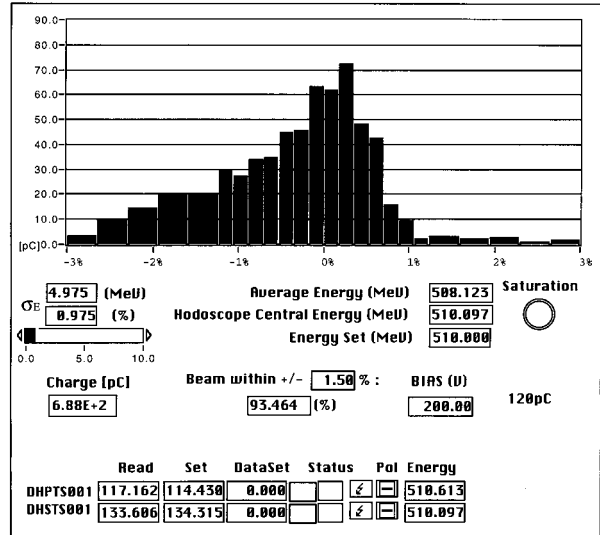


Figure 3: Energy distribution of the positron beam.

The RF Linac scheme allows to operate in the positron mode with the CS RF phase in 2 different configurations: accelerating and decelerating field. It has been evidenced [7] that in the decelerating mode a significant gain in the positron capture should be obtained at the cost of a small loss in energy.

Figure 4 shows some preliminary measurements of this effects performed on the DAΦNE Linac. Currently, the CS is used in the accelerating mode.

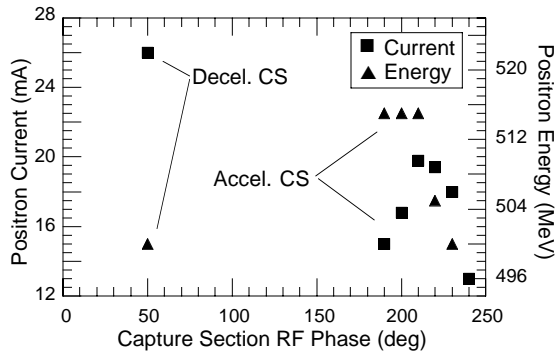


Figure 4: e^+ current & energy vs CS RF phase.

4 ELECTRON MODE RESULTS

In the electron mode of operation the PC target is extracted, the flux concentrator and the separator are turned off, the electron gun output current is drastically reduced and the output power coming out from the klystrons is diminished.

Figure 5 shows the electron beam current along the Linac during a typical run. From left to right 565 mA are present at the gun output, 350 mA at the PC, 325 mA after the separator and 297 at the Linac end.

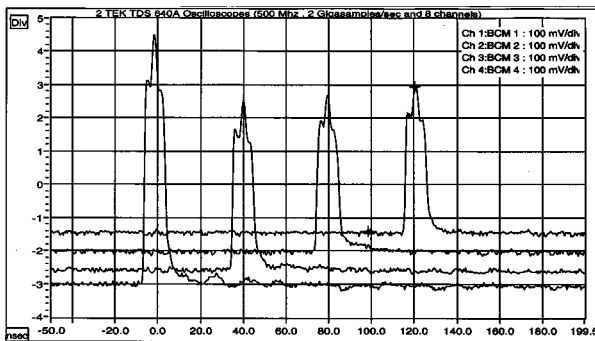


Figure 5: Current monitor signals in electron mode.

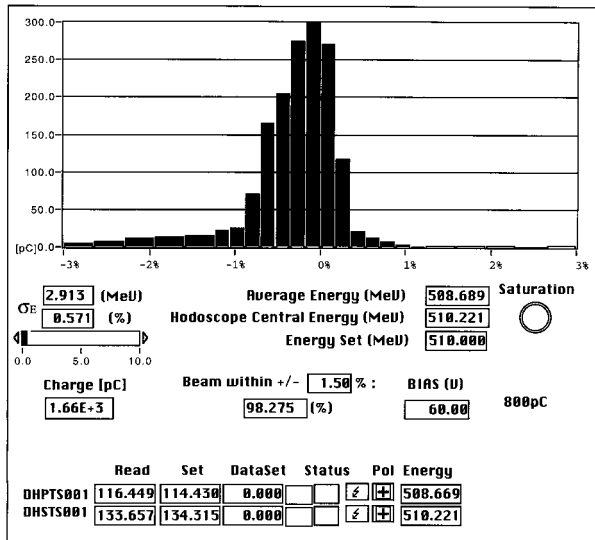


Figure 6: Energy distribution of the electron beam.

The electron beam energy distribution is shown in Figure 6. It can be seen that the rms spread is 0.57 % and that practically all the beam is within the acceptance of the downstream transfer line and Accumulator ring.

It must be said that macrobunch currents of up to 1 A at the Linac end have been obtained with the electron beam. Anyway such a current values cannot be used because the beam loading inside the accelerating sections generates an increase of the energy spread (3 % rms with 1 A) beyond the transfer line and Accumulator acceptance.

5 CONCLUDING REMARKS

As part of the DAΦNE injector, the major requirements to the Linac come from the positron mode of operation. As already said, the good results obtained with the positron beam permit to reduce the DAΦNE injection time with beneficial effects on the integrated luminosity.

After a total of about 300 days of 24 hours/day operation shifts, all the Linac subsystems are completely debugged and the reliability level achieved is quite satisfactory. The fault statistics indicate in the gun pulser and in the modulator PFN capacitors the principal sources of faults. The reasons of these faults have been understood and actions for fixing them are being adopted.

ACKNOWLEDGMENTS

The achievement of the described results has been made possible to great extent thanks to the continuous and professional work performed by the LNF technical staff involved in the Linac operation. The authors want to express their appreciation to M. Belli, A. Cecchinelli, R. Clementi, E. Grossi, M. Martinelli, V. Pavan, R. Pieri, G. Piermarini, and R. Zarlenga.

Special thanks also to M. Giabbai and P. Possanza for the patience and accuracy used in editing this paper.

REFERENCES

- [1] C. Biscari, "Performance of DAΦNE", this Conference.
- [2] M.E. Biagini et al., "Performance and operation of the DAΦNE Accumulator", this Conference.
- [3] K. Whitham et al., "Design of the e^+/e^- Frascati Linear Accelerator for DAΦNE", PAC 93, Washington, May 1993.
- [4] F. Sannibale, M. Vescovi, R. Boni, F. Marcellini, G. Vignola, "DAΦNE Linac commissioning results", DAΦNE Technical Note BM-2, April 1997.
- [5] F. Sannibale, M. Vescovi, "Linac to Accumulator area transfer line & DAΦNE Linac spectrometer", DAΦNE Technical Note LC-3, February 1992.
- [6] F. Sannibale, "DAΦNE Linac beams emittance measurement design", DAΦNE Technical Note LC-5, September 1992.
- [7] B. Aune, R.H. Miller, "New method for positron production at SLAC", SLAC-PUB-2393, September 1979.

PERFORMANCE AND OPERATION OF THE DAΦNE ACCUMULATOR

M.E. Biagini, C. Biscari, R. Boni, V. Chimenti, A. Clozza, S. De Simone, G. Di Pirro, A. Drago, A. Gallo, A. Ghigo, S. Guiducci, F. Marcellini, M.R. Masullo, C. Milardi, L. Pellegrino, M.A. Preger, C. Sanelli, F. Sannibale, M. Serio, F. Sgamma, B. Spataro, A. Stecchi, A. Stella, G. Vignola, M. Zobov, LNF-INFN, Frascati, Italy

Abstract

DAΦNE [1] is an electron/positron collider, in operation at INFN Frascati since the beginning of 1998. Its injection system [2] consists of a 0.55 GeV positron (0.8 GeV electron) Linac, an intermediate damping ring, called "Accumulator", and ≈ 180 m long Transfer Lines connecting the Linac to the Accumulator and the Accumulator to the collider Main Rings. The Accumulator is a 0.55 GeV storage ring, operating in the single bunch mode, where electrons and positrons accelerated by the Linac are alternatively captured and stacked with high efficiency, due to its large acceptance and short damping time. The high quality damped beam is then extracted and transferred to the collider. The whole injection system has been designed to fill the Main Rings in few minutes. The operating experience with the Accumulator has demonstrated the feasibility of this goal.

1 INTRODUCTION

Among several projects of electron-positron "factories", namely high luminosity colliders running at the peak of high cross section resonances, DAΦNE [1] is presently under commissioning at INFN Frascati. The appellation "factory" for a collider comes from the peculiar characteristic of being capable of producing an extremely high rate of a given type of particles. In the case of DAΦNE, the particles are K mesons from the decay of the Φ resonance ($\approx 5 \cdot 10^3$ nb at 1.02 GeV c.m.).

The design luminosity of DAΦNE is $5 \cdot 10^{32}$ cm⁻²s⁻¹. This value exceeds by almost two orders of magnitude the maximum luminosity achieved at the same energy (0.51 GeV per beam) at the VEPP-2M collider of Novosibirsk [4]. This strong improvement is obtained by realizing the collider as a double ring structure with two low- β interaction regions where the counterrotating beams cross at a small angle in the horizontal plane. With this arrangement it is possible to store in each ring a large number of bunches (up to 120), each crossing the other beam only in the two interaction regions. With respect to a single ring collider, where, unless the beams are separated at the high- β crossing points by means of electrostatic separation schemes, the maximum number of bunches is half the number of low- β interaction regions (typically 1 or 2 in such low energy range), the luminosity can therefore be improved proportionally to the number of

stored bunches. The limitation on this number comes from the minimum bunch spacing, determined by the crossing geometry and the minimum separation required between bunches of the opposite beams at parasitic crossings near the interaction points.

It is clear that this double ring scheme with many bunches requires a very large average stored current in each ring. In the case of DAΦNE the design value for the maximum current is ≈ 5 A.

The beam lifetime at low energy is dominated by the Touschek effect: it is estimated to be ≈ 2 hours in the design configuration of the beam. Flexible operation of the collider requires injection of any bunch pattern, at least in the commissioning stage, so that it should be possible to store each bunch individually in the rings. A very powerful injection system, running in the single bunch mode at the operation energy of the collider is therefore required to fill the Main Rings from scratch at full current in few minutes. With such a system, the rings can also be refilled without dumping the stored beam, keeping the average luminosity of the collider very close to the maximum one.

2 DESIGN PHILOSOPHY

The RF bucket width in the DAΦNE Main Rings is 2.7 ns. With the maximum positron current available from the Linac [2] (≈ 7 0 mA positrons and 300 mA electrons), $\approx 10^4$ injection pulses would be necessary to fill the positron ring. With such a large number of pulses, strict requirements on the injection aperture are mandatory to avoid saturation. With an intermediate booster between the Linac and the collider this large number can be split into two factors, the number of injection pulses into the booster (≈ 80 for the same longitudinal acceptance and full efficiency) to reach the full current of a single Main Ring bunch times the number of bunches (120).

There are two additional important advantages of this choice:

- the RF system in the booster can run at a lower frequency, thus improving the longitudinal acceptance (in our design the frequency is 5 times lower, thus reducing the number of injection pulses into the booster from ≈ 80 to ≈ 15 at full efficiency).
- it is possible to damp the beam in the booster before extraction: in this way the beam quality (emittance and energy spread) is typically one order of magnitude better

than the corresponding one of a beam accelerated by a Linac at the same energy, thus substantially reducing the aperture requirements in the collider.

The booster, called "Accumulator", has been designed under the following constraints:

- reference orbit length exactly 1/3 of the DAΦNE Main Ring one to allow easy synchronization;
- symmetric structure to allow injection/extraction of both electron and positron beams without changing the magnetic fields;
- low emittance and energy spread, short damping time;
- low dispersion in the injection/extraction sections.

These requirements are fulfilled by designing the lattice as a symmetric structure of four quasi-achromatic sections, each one with two small radius (1.1 m) dipoles with a field index of 0.5 and three quadrupoles [3], separated by long straight sections to accommodate the injection/extraction septa, the kicker magnets and the RF cavity. The chromaticity is corrected by means of 8 sextupoles, 2 in each achromat. The Accumulator layout is shown in Figure 1.

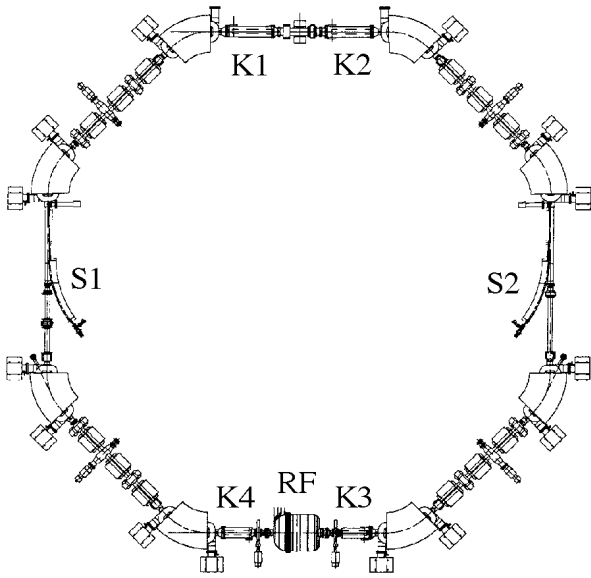


Figure 1: Accumulator layout

Positrons are injected at 50 Hz through septum S1 by a symmetric closed bump generated by the four kickers. When the full single bunch current (≈ 130 mA) is reached, the beam remains stored for 5 damping times to reach its equilibrium emittance and energy spread. The beam is then extracted through septum S2 by means of a single pulse in kickers K1 and K2. The whole cycle requires typically one second. The electrons follow the opposite path, being injected through S2 and extracted through S1. In such a way the ring is operated in a steady configuration.

The horizontal betatron tune of the ring has been adjusted to obtain the correct phase advance between kickers and injection septa for both beams and to have a small

average dispersion in the straight sections and bending magnets. Both tunes are slightly above the integer to avoid resistive wall instability. Figure 2 shows the optical functions of 1/4 of the ring. The structure of half ring is obtained by mirror symmetry and the full lattice by repeating the sequence. Table 1 lists the main parameters of the Accumulator.

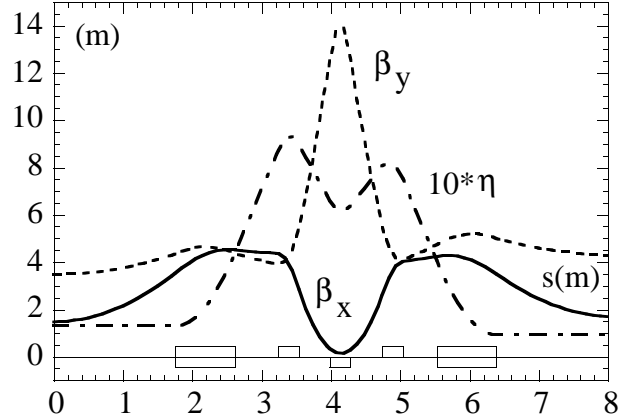


Figure 2: Optical functions of 1/4 of the ring

Table 1: Accumulator parameters

Energy (GeV)	0.51
Circumference (m)	32.56
Maximum single bunch current (mA)	132
Horizontal betatron wavenumber	3.12
Vertical betatron wavenumber	1.14
Horizontal betatron damping time (ms)	21.4
Vertical betatron damping time (ms)	21.4
Synchrotron damping time (ms)	10.7
Momentum compaction	0.04
Emittance (mm.mrad)	0.25
Energy spread (% , rms, radiation only)	0.04
RF frequency (MHz)	73.65
RF voltage (KV)	200
Radiated energy per turn (keV)	5.2
Energy acceptance (%)	$>\pm 1.5$
Bunch length (cm, rms, radiation only)	1.8

3 OPERATING EXPERIENCE

The Accumulator construction was completed in December 1995. After completing the installation of the Transfer Line from the Linac inside the Accumulator Hall and the electric and cooling systems, commissioning of the ring was easily and rapidly performed. The first electron beam was stored in June 1996. The first positron beam was stored and extracted in November 97, and design performance with both beams achieved at the beginning of 1998. In the commissioning phase the Linac runs at half the nominal repetition rate, and ≈ 50 mA positrons are

routinely stacked at 25 Hz in less than one second in a single bunch. The design current corresponding to the required charge per bunch in the Main Rings (132 mA) can be easily reached. The maximum single bunch current stored under stable conditions exceeds 150 mA. The lifetime of the stored beam is largely sufficient for injection into the Main Rings, being more than half an hour at the maximum operating current.

The operation of the Accumulator for the collider commissioning is reliable and downtime negligible.

Figure 3 shows the output of a DC beam current transformer during a typical injection/extraction cycle with electrons for the commissioning of the Main Rings. In this configuration 5 electron pulses are stored in the Accumulator; then the beam is damped and extracted. The repetition rate of this sequence is 1 Hz.

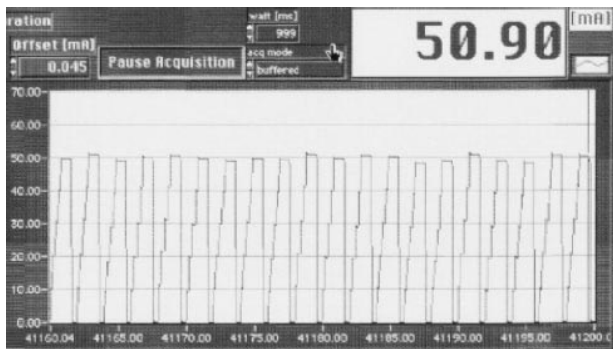


Figure 3: A typical injection/extraction cycle as seen on the DCCT monitor

The overall injection time into DAΦNE depends critically on the injection efficiency of the positrons, since the electron current from the Linac is so large that the injection rate of the electrons is limited by the maximum repetition rate of the pulsed elements in the Transfer Line. The overall transport and capture efficiency from the Linac to the Accumulator for positrons is $\approx 40\%$. The loss takes place mainly in the Transfer Line due to the fact that we do not use any energy selecting slit at the Linac output. The capture efficiency itself, defined as the stored beam current divided by the beam current at the first revolution inside the Accumulator is 95%. The overall efficiency for electrons is 60%. There is still some margin for improvement in the injection efficiency, since the achieved rates are largely sufficient for the commissioning of DAΦNE, and no machine time was dedicated to the optimization of the injector performance.

The extraction efficiency is defined in a similar way and, due to the small emittance and energy spread of the damped beam, it is close to 100%.

The shift of the synchronous phase and the bunch length have been measured as a function of the current stored in a single bucket of the Accumulator [5]. Due to the high RF frequency of the Main Ring cavities (368.26 MHz) required to store a large number of

bunches, injection efficiency into the Main Rings could be affected by bunch lengthening at high current. This is not the case, as it can be seen from Figure 4, showing the result of the measurement: the maximum FWHM bunch length is ≈ 17 cm, to be compared with the Main Ring bucket length of 81 cm. By fitting the measured bunch length values with a standard model [6], the low frequency longitudinal coupling impedance $|Z/n|_0$ comes out to be 3.55Ω , in good agreement with the predictions of the numerical simulations which take into account the shape of the vacuum chamber discontinuities.

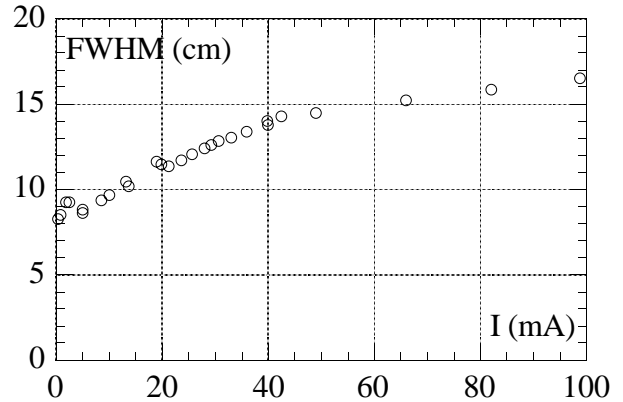


Figure 4: Bunch length versus average current between 60 and 90 KV in the R.F. cavity.

The transverse coupling impedance has also been measured [7]: its value of $70 \text{ K}\Omega/\text{m}$ agrees with the predictions of the simulations. A conservative estimate for the threshold of the transverse mode coupling instability comes out to be 160 mA, larger than the single bunch current in the Accumulator required to fill the maximum design current in each bunch of the DAΦNE Main Rings.

REFERENCES

- [1] C. Biscari, DAΦNE Team "Performance of DAΦNE", this Conference.
- [2] R. Boni et al. "DAΦNE Linac operational performance". this Conference.
- [3] H. Hsieh et al. "Magnetic Measurements of the Dipole, Quadrupole and Sextupole Prototypes for the Accumulator of DAΦNE, the Frascati Φ-factory", EPAC'96 p. 2182.
- [4] L.M. Barkov et al "Status of the Novosibirsk Φ-Factory Project" PAC'91, p.183.
- [5] R. Boni et al. "Bunch length and phase shift measurements on DAΦNE Accumulator" DIPAC'97, LNF-97/048 (IR) p. 174.
- [6] A.W. Chao and J. Gareyte "Scaling laws for bunch lengthening in SPEAR II, SPEAR-197 (1976).
- [7] M. Zobov et al. "Transverse mode coupling instability in the DAΦNE Accumulator Ring", DAΦNE Technical Note G-50 (22/5/1998).

DAΦNE MAIN RING OPTICS

M. Bassetti, M.E. Biagini, C. Biscari, S. Guiducci, M.R. Masullo,
C. Milardi, M.A. Preger, G. Vignola, LNF-INFN, Frascati, Italy

Abstract

DAΦNE [1] is the $e^+ e^-$ Φ-Factory presently under commissioning at INFN Frascati. The two beams have been successfully injected and stored and the optics has been tuned to operate in collision mode. The optics solutions adopted to solve the problems set by the requirements of a high intensity, high luminosity Φ-Factory are described. Preliminary measurements of the optical parameters are presented and compared with a machine model.

1 INTRODUCTION

In order to reach the high design luminosity at the low c.m. energy of the Φ (1.02 GeV) the scheme of a double ring collider with a maximum number of 120 bunches per ring has been chosen. The beams collide in two 10 m long Interaction Regions (IRs) at a crossing angle in the horizontal plane.

Particular care has been taken in the design to make the damping times as short as possible in order to counteract any harmful instability in such low energy range. Low bending radius in the dipoles and 4 high field wigglers in each ring produce large energy loss (9 KeV per turn).

A peculiar feature of the lattice is the Interaction Region (IR) where the two beams travel together in a common vacuum chamber. Due to the crossing angle in the horizontal plane, the beams pass through the low-β quadrupoles off axis. A correction scheme with the splitter magnets [1] and corrector dipoles allows to change the crossing angle so that the effect of parasitic crossings can be finely tuned.

Two large detectors, each one equipped with a longitudinal field solenoid, will be installed at the Interaction Points (IPs). Due to the large free solid angle required by the experiments, the low-β triplets are realized with permanent magnet quadrupoles. At this stage of DAΦNE commissioning the two low-β interaction regions are operated without solenoidal fields and with conventional electromagnetic quadrupoles.

2 MAIN RINGS LATTICE

2.1 General layout

The Main Rings layout is shown in Fig. 1. Each ring is divided in two sectors, an outer one, called Long, and an inner one (Short) each one symmetric with respect to its own center.

The lattice consists of 4 achromats (called arcs in the following), each housing: three quadrupoles, a 2 m, 1.8 T

normal conducting wiggler and 2 chromaticity correcting sextupoles between two bending magnets. The quasi-achromatic structure of the cell allows for vanishing dispersion at the Interaction Points (IPs) and in the R.F. cavity. One of the dipoles has parallel end caps providing vertical focusing in order to obtain well separated optical functions at the sextupoles. The wigglers run always at top field to obtain strong damping. Moreover, by changing the dispersion inside the wigglers, it is possible to tune the emittance to large values (an order of magnitude larger than the contribution from the dipoles). This kind of cell has been tested successfully for the first time in a storage ring and we call it BWB.

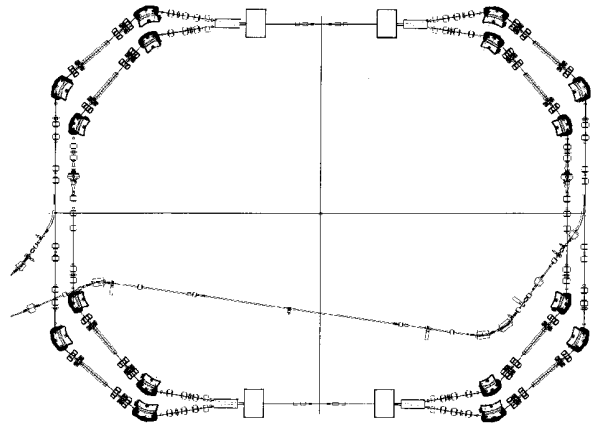


Figure 1: Layout of DAΦNE Main Rings.

Injection kickers, RF cavity and longitudinal feedback are housed in the straight sections orthogonal to the IRs. Outside the arcs 8 sextupoles are used to correct the tune shifts with amplitude and momentum. Eight skew quadrupoles are installed in each ring to control coupling.

The optical functions of the Long and Short sectors have been designed as much as possible similar, even if there is no symmetry with respect to the IPs. Non vanishing dispersion in the injection region is used to obtain large momentum compaction, improving the threshold for microwave instability. Due to the low energy spread of the beams coming from the Accumulator [2] injection efficiency is not affected by this dispersion.

The betatron tune working point has been chosen on the basis of beam beam simulations [3]. In order to have the maximum flexibility each quadrupole is individually powered. Anyway the tunes can be varied on a large range by changing the quadrupole settings only in the Short straight section, leaving the optical functions in the rest of the ring unchanged.

The single ring parameters are summarised in Table 1.

Table 1: DAΦNE Single Ring Parameters

C (m)	97.7	β_x^* (m)	4.5
F_{rf} (MHz)	368.26	β_y^* (m)	.045
h	120	κ	.01
ϵ (m*rad)	10^{-6}	σ_x^* (m)	$2.1 \cdot 10^{-3}$
θ (mrad)	20÷30	σ_y^* (m)	$2.1 \cdot 10^{-5}$
α_c	.02	σ_E^{nat}	$4 \cdot 10^{-4}$
U_o (keV/turn)	9.3	τ_x (ms)	36.

2.2 Interaction Regions

The IRs are a large fraction of the ring circumference ($\approx 20\%$). The optical functions are symmetric with respect to the IP. The beams travel off axis in the IRs, being separated at the IR ends by about 12 cm. To increase the separation and to lower the chromaticity, mainly due to the low- β insertions, a focusing sequence FDF has been chosen. The IR modelling [4] takes into account the linear effects of the fringing quadrupole fields on the off axis trajectories.

Four different IR lattices have been designed: three for the experiments and one for commissioning. The total IR first order transport matrix is nearly the same for all configurations, thus allowing to interchange the four IRs with small adjustments of the optical functions in the arc.

The large detector solenoids are a strong perturbation to the machine optics (BL = 2.4 Tm) and give the major contribution to the coupling. A sophisticated compensation scheme has been designed [5].

For machine commissioning the DAY-ONE IR houses seven electromagnetic quadrupoles, to allow tuning of the optical functions, with a quadrupole placed at IPs. This scheme reduces the chromaticity. A Beam Position Monitor (BPM) at the IPs allows to align the two beams for the colliding configuration.

3 OPTICS MEASUREMENTS

Commissioning started with the nominal β^* .

The first working point was far from the integer ($\nu_x = 5.14, \nu_y = 5.21$) to reduce closed orbits and make

first injection and storage easier. In order to optimize the luminosity, the working point has been then moved closer to the integer ($\nu_x = 5.11, \nu_y = 5.07$). Injection has been optimized and measurements to characterize the ring lattice have been performed on this working point as well.

3.1 Lattice Modelling

Due to the high beam emittance the machine aperture is large; for this reason and because of the short lengths of the magnetic elements the effect of the fringing fields is not negligible and a correction to the rectangular model has been applied for most of them. The edge effect of the dipole is represented by a thin lens on each side with a focusing strength computed from magnetic measurements. This effect accounts for a change of almost 0.5 in the vertical tune. The wiggler magnets are modelled by a sequence of parallel face dipoles, taking into account also the focusing effect of the sextupole field component on the oscillating trajectory whose amplitude is ≈ 3 cm.

The measured tunes on the first stored beam were in agreement with those calculated with this preliminary model within 0.05.

The horizontal and vertical β functions along the rings have been measured by recording the change in tunes given by a variation of the current in each quadrupole. As an example, Fig. 2 shows the comparison between measured and computed β functions for the e^- ring. The model fits quite well the measurements for different tunes. The computed emittance agrees with the design value within 10%.

3.2 Closed orbit

The closed orbit measurement, available under the DAΦNE Control System [6], provides the beam position in real time. Four methods to correct the closed orbit have been implemented:

- best corrector
- harmonic correction [7]
- eigenvalues of measured response matrix
- bumps in the IRs.

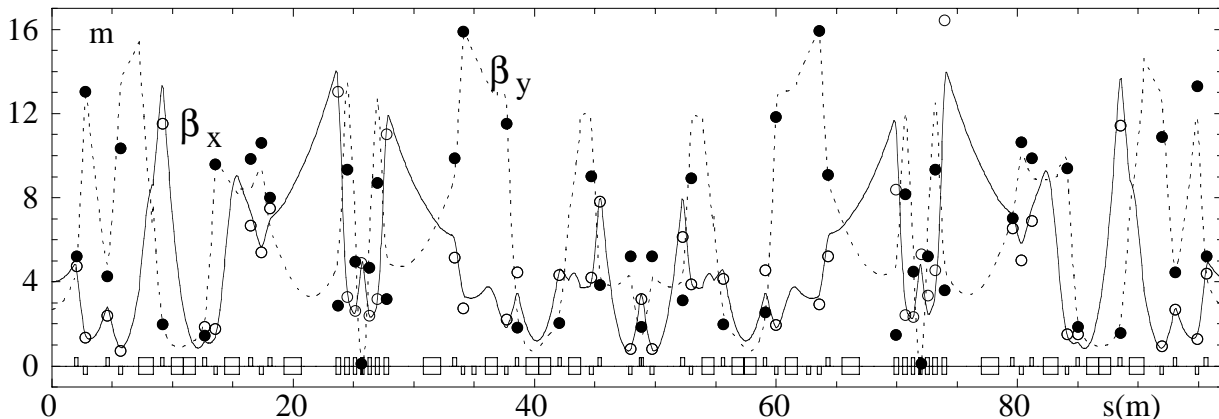


Figure 2: Horizontal and vertical β functions in one ring. White and black dots are measured β_x and β_y respectively.

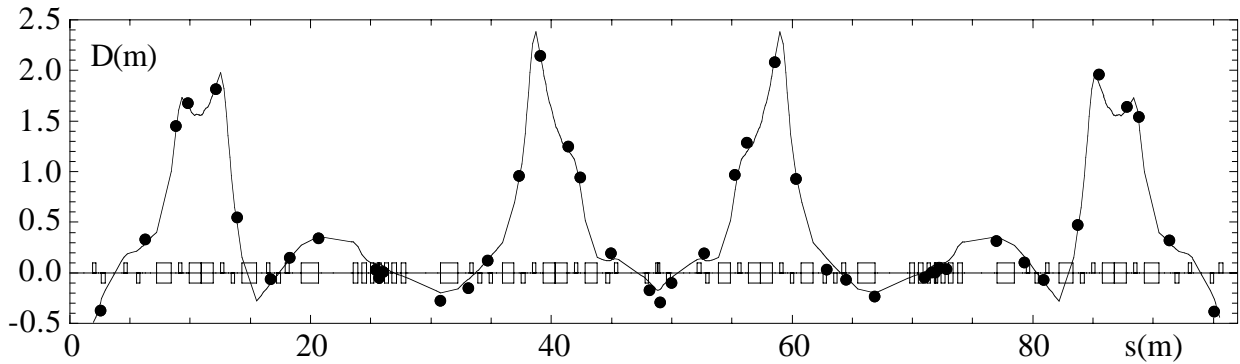


Figure 3: Horizontal dispersion function in one ring. Dots are measured values

Orbit bumps in the IRs, with four correctors, have been used to precisely adjust angle and displacement in the horizontal and vertical plane at the IP. The orbit measurement in the IRs is performed separately for each beam in the same monitors and therefore the superposition of the two beams is not affected by monitor offsets. Bumps are also used to vertically separate the beams in one IR when colliding in one IP only.

The Response Matrix of the ring, giving the beam position in all BPMs versus the perturbations in corrector magnets, has been measured. It has been used to check the machine model as well as for calibration of the corrector strengths.

Since the two rings are very close to each other, there is magnetic cross-talk between the two rings. Fringing fields from high field elements produce orbit changes on the nearby ring. These effects have been corrected. The horizontal closed orbit is determined not only by magnetic misalignments, but also by the compensation of the trajectory in the wigglers and by the splitter setting as a function of the crossing angle at the IP. The closed orbit without correctors is within the aperture in both rings.

The dispersion function, shown in Fig. 3, has been measured from closed orbits at different RF frequencies. Coupling has been estimated from the beam image given by the Synchrotron Light Monitor [8] for both beams. Closed orbit correction has led to κ values around 0.03. Skew quadrupoles have been adjusted reaching the coupling design value of 0.01.

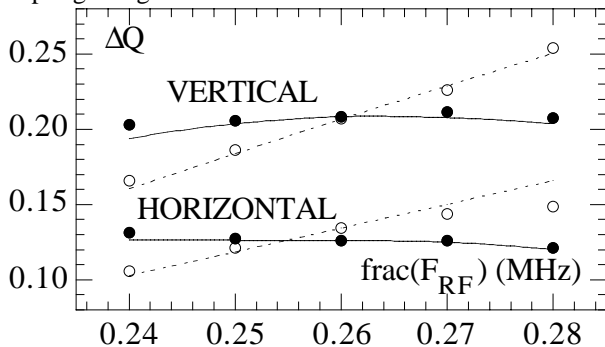


Figure 4: Measured (dots) and computed (lines) chromaticity with (black) and without (white) sextupoles

3.3 Chromaticity

Fig. 4 shows the comparison between theoretical (lines) obtained from a tracking code and measured (dots) horizontal and vertical chromaticities for the e^- ring, with and without sextupoles, performed on the working point (5.14, 5.21). The agreement is pretty good up to energy deviations of the order of $\pm 0.5\%$. The difference in horizontal tune with and without sextupoles at the central RF frequency is due to closed orbit in the sextupoles.

4 CONCLUSIONS

The optics measurements described here have been useful to establish a machine model to adjust the operating point and to tune the lattice for the two beams operation. The closed orbit in the rings is small enough to obtain design coupling with sextupoles on. More accurate modelling for two beams operation is proceeding in parallel with the commissioning.

REFERENCES

- [1] C. Biscari, DAΦNE Team, "Performance of DAΦNE", these proceedings.
- [2] M.E.Biagini et al, "Performance and operation of DAΦNE Accumulator", these proceedings.
- [3] K. Hirata, M. Zobov, Proc. of EPAC 96, Spain, June 1996, p. 1158.
- [4] M. Bassetti, C. Biscari, "Effects of fringing fields on single particle dynamics", 14th ICFA Beam Dynamics Workshop, Frascati, Oct. 1997.
- [5] M. Bassetti, et al, "Solenoidal field compensation", 14th ICFA Beam Dynamics Workshop, Frascati, Oct. 1997.
- [6] G. Di Pirro et al, "The DAΦNE Control System Status and Performance", these proceedings.
- [7] M. Bassetti, S. Guiducci, "Harmonic closed orbit correction with the Lagrange multipliers method", DAΦNE Technical Note G-46, April 1997.
- [8] A. Ghigo et al, "Synchrotron Radiation Monitor for DAΦNE", AIP Conf. Proc. No.333, p. 238, Oct. 1994.

DAΦNE CONTROL SYSTEM STATUS AND PERFORMANCE

G. Di Pirro, A. Drago, G. Mazzitelli, C. Milardi, F. Sannibale, A. Stecchi, A. Stella,
LNF-INFN, Frascati, Italy

Abstract

The DAΦNE Control System allowed the step by step commissioning of the major subsystems as they were installed, proving to be modular and extensible. Recently the guidelines of the Control System evolution concerned the development of machine operational procedures and the integration of diagnostic tools. Particular attention has been reserved to the problem of saving and restoring element data sets as well as to the DAΦNE general data handling. A system overview including installation status, features, and operation results is presented.

1 INTRODUCTION

The Main Rings of DAΦNE [1], the e^+e^- Frascati Φ-factory, are under commissioning since September 1997 when the mechanical installation was completed. At the present all the efforts are aimed at pushing up the performance of the accelerator complex as a whole since it is expected to provide a luminosity:

$$L = 1.3 \cdot 10^{32} \text{ cm}^{-2} \text{ sec}^{-1}$$

the highest ever reached at the working energy $E = 510 \text{ MeV}$.

The Control System [2] for DAΦNE is completely and uniformly based on personal computers.

The choice of commercial software such as LabVIEW® [3] at all levels and the development of specific hardware, based on Macintosh™ boards in a VME environment, succeeded in the development of a Control System suitable for machine operation. The Graphical User Interface provides friendly interaction with single machine elements and complex accelerator oriented procedures. The machine devices are driven by many distributed CPUs. A shared memory instead of a network permits fast, straightforward and high bandwidth communications.

The DAΦNE Control System architecture is well established. Important subsystems such as RF and timing, but also many basic diagnostic tools have been integrated in the Control System and run routinely. All the 462 independent power supplies of the DAΦNE magnets can be remotely operated through the Control System user interface.

A summary view of the control system installation status is reported in Figure 1.

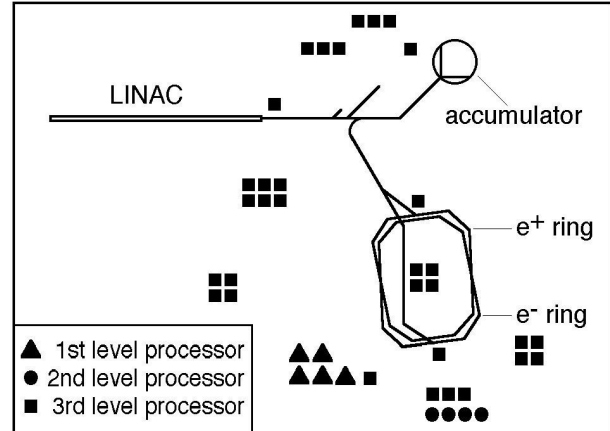


Figure 1: Distribution of processors over the accelerator area. The 3-rd level processors (squares) are located close to the related elements in order to minimize the wiring of local connections. The 2-nd level processors (circles) are located in the central cluster of VME crates where all the commands and messages flow. The 1-st level processors (triangles) are located in the control room.

2 OPERATIONAL PROCEDURES

Looking for the best DAΦNE working point, operations such as beam injection, betatron tuning, closed orbit correction and machine setups saving are quite usual. These operations have to be performed in automatic mode otherwise they become heavily time consuming and can compromise the commissioning.

2.1 e^+e^- Switch Procedure

In DAΦNE e^-e^+ beams are accelerated in different Main Rings sharing only the two Interaction regions. However they are supplied by the same injection system that consists of a LINAC, a booster ring, the Accumulator [4] and a complex Transfer Line. Although some Transfer Line sections are specific for a given beam, the largest part is shared by e^+ and e^- , which somewhere run both ways. A timing system [5] synchronizes the pulsed magnets in the Transfer Lines and the kickers in Accumulator and Main Rings providing the right path to each kind of particle.

Due to the DAΦNE characteristic beam life time $\tau = 2 \text{ h}$ the Injection System is expected to switch often and quickly between e^+ and e^- operation mode. This requirement is even tighter during the commissioning when frequent beam losses occur.

For these reasons an automatic switch procedure has been implemented. It is based on the Command Recorder which is a general Control System tool able to record and play back a command sequence learning from the operator action. Using the Command Recorder and loading proper command files the operator can change, with a single action, polarity, setpoint and delay time for all the elements in the Injection System and after a couple of minutes the required beam is available on the proper injection septum.

2.2 Magnet Synchronization

During machine operations it is important to move synchronously the setpoint of a certain number of magnetic elements.

It allows, for instance, to tune the machine optics, to correct the stored beam orbit and to realize local bumps at the interaction regions.

An user interface program allows to load a precompiled file containing the names of the involved elements with their setpoints. The file can be loaded as absolute settings or relative variations as well and the target values can be further modified from the control window. The user enters the number of steps to be used to reach the final working point and then operates two "Forward" and "Reverse" arrow buttons. Each time either button is pressed, the application issues the corresponding bunch of commands with the calculated delta sets for the current steps and monitors the actual readbacks.

In the present version the synchronization is determined by the system software latency time and by the serial communication protocol with the magnet power supplies. The former is much shorter with respect to the second one, which is of the order of tens of ms. In addition to the starting time uncertainty, no simultaneity of current ramps is guaranteed by any means.

In order to get a tighter synchronization the commands PSET and SSLP have been introduced. They preset the desired setpoint and slewrate on a power supply, at this point a TTL pulse, sent to all the power supplies, triggers the start of the current ramp. This "hardware synchronization" has been successfully tested and will be soon operative.

2.3 Save & Restore

The capability to store and recover from disk data corresponding to a certain machine working condition is a primary service that any control system must provide.

During the first commissioning phase it has been decided to adopt a save and restore mechanism based on the concept of operating areas.

The DAΦNE complex has been fragmented into many subsets such as: Accumulator Injection, Accumulator, Accumulator Extraction, and so on.

Each area is in turn structured by element classes which leads to a highly modular file structure.

Dealing with more general framework, the save and restore services have been redesigned including much larger areas that can be stored both as single datasets or as belonging to a general machine configuration. Custom dataset files of elements belonging to different classes and machine areas are still possible.

This new structure is under test and is going to replace the previous ones.

3 DATA HANDLING TOOL

Data in the Control System consist of a large amount of information written into the VME memory in a wide range of different formats. Usually data are fetched by specialized control windows, but the correlation of data all over the accelerator is more complicated.

A process has been developed fetching all the different front-end devices and aligning all the information in a universal format Data Base. This allows to have an on-line uniform memory refreshed with a settling time. The process also dumps data of interest on storage disk for off line and long term analysis.

Based on this on-line data base many diagnostic tools have been implemented such as the "Hunter Dog" task that allows to check the status of all the machine elements, alerting the operator of any possible failure.

4 DIAGNOSTICS

The beam position measurements are fully integrated in the Control System. At the present two different systems are running. One of them is mainly for Trajectory measurements and is used to monitor the beam along the Transfer Line, the first turn in the Main Rings and the first turn and the orbit in the Accumulator. The other one has been designed to measure the stationary closed orbit in the Main Rings and works with stored beam only.

Another primary diagnostic is the Luminosity monitor since it provides an ultimate check of the whole complex tune-up.

4.1 Beam Orbit Measurements

The Trajectory measurement relies on a hardware setup including an RF multiplexer system used to select the four channels of each Beam Position Monitor (BPM), mainly strip line, as inputs for a digital scope TDS 644/A by Tektronix, used to read the voltage signals. A user interface window allows to load the BPMs in the machine section of interest, to configure the digital scope at run time as well as from a file and to acquire the trajectory in one shot or reading a BPM selected by the operator, that is much more useful during the Transfer Line optimization. The beam trajectory is displayed on the interface window in both planes together with the sum over all the pickup signals for each BPM. This number is proportional to the beam current and provides an immediate feeling of the transmission efficiency.

4.2 Beam Position Measurements

The closed orbit measurement in the Main Rings [6] is based on four parallel processors each of them dealing with one fourth of the involved BPMs. The BPM outputs are converted in a couple of DC signals proportional to the horizontal and vertical beam position by Bergoz BPM modules [7]. Then they are acquired using a digital voltmeter and after a linearization process stored as beam positions, at the rate of 5/sec, on a 1 Mbyte circular VME memory available on each processor. Since each beam orbit is spread among four different buffers, all the acquisitions are labeled by a header specifying the date and time and an acquisition progressive number.

The accuracy of the whole orbit acquisition system has been measured. At low current the rms beam position error is inversely proportional to the beam current, then it approaches asymptotically about 0.02 mm above a threshold current $I \approx 3$ mA.

The beam closed orbit is displayed on the Control System user interface by a dedicated window. The operator can decide to visualize only the last orbit or to display up to ten sequential orbit at the same time. A reference orbit can be subtracted from the one presented on the screen. The reference can be chosen among previously saved orbit files or orbits captured at run time in the interface window, which provides a buffer where up to ten reference orbits can be held. Moreover, the operator can decide to stop the orbit monitoring and to look back to past orbits stored in the processor memory buffers.

This diagnostic tool has been particularly useful in the first stage of the DAΦNE commissioning since it pointed-out slow drifts and glitch problems in some magnets.

4.3 Luminosity Monitor

An essential diagnostic tool is the luminosity monitor [8].

The detector consists of a sampling lead-scintillating fiber calorimeter, equipped with a photomultiplier read-out measuring the high counting rate of the single bremsstrahlung (SB) events at the interaction point. The calibration procedure, based on gas bremsstrahlung (GB) analysis, allows to measure the energy cut-off and the resolution. The calibration chain, based on charge ADC CAEN V265 in VME, allows a fast on-line GB spectra analysis up to 1KHz.

Several calibration and measurement procedures have been developed and integrated in the control system.

The counting chain in the luminosity measurement setup is based on a VME scaler STRUCK str7200 counting the rate of GB noise and the SB signal at the two interaction points in many different configurations.

5 MEASURED RESPONSE MATRIX

Data from beam closed orbit have been used to build an user interface process allowing to measure the machine Response Matrix in a short time, three minutes. The Response Matrix is made up by columns where the orbit variation corresponding to a given perturbation is stored. Perturbations are provided by varying the strength of correction magnets, quadrupoles and sextupoles.

The measured Response Matrix is extensively used for machine modelling and beam closed orbit correction.

6 CONCLUSIONS

The DAΦNE Control System is running for three years. Its general structure has been tested in the overloading commissioning environment and it proved to be suitable and reliable. Many important diagnostic tools and operational procedures have been provided and have been useful both in commissioning DAΦNE and in pointing out subsystem faults.

7 ACKNOWLEDGMENTS

Thanks are due to the DAΦNE Team for continuous stimulating discussions and to Gianfranco Baldini and Mario Masciarelli for their unlimited technical support in the DAΦNE Control System realization.

REFERENCES

- [1] "DAΦNE Performance", by C. Biscari and DAΦNE Team, this Conference.
- [2] "DANTE: control system for DAΦNE based on Macintosh and LabVIEW", by G. Di Pirro, C. Milardi, A. Stecchi and L. Trasatti, Nuclear Instruments and Methods in Physics Research A 352 (1994) 455-475.
- [3] LabVIEW® National Instrument Corporation, 6504 Bridge Point Parkway, Austin, TX 78730-5039.
- [4] "Performance and operation of the DAΦNE Accumulator", by M.E. Biagini et al., this Conference.
- [5] "Implementation and Performance of the DAΦNE Timing System", by A. Drago, G. Di Pirro, A. Ghigo, F. Sannibale, M. Serio, this Conference.
- [6] "Integration of Diagnostics in the DAΦNE Control System", by G. Di Pirro, A. Drago, G. Mazzitelli, C. Milardi, M. Serio and A. Stecchi, DIPAC 97 67-69.
- [7] Beam Position Monitor, BERGOZ Precision Beam Instrumentation 01170 Crozet, France.
- [8] "The DAΦNE Luminosity Monitor", by G. Di Pirro, A. Drago, A. Ghigo, G. Mazzitelli, M. Preger, F. Sannibale, M. Serio, G. Vignola, F. Cervelli and T. Lomtadze, 8th Beam Instrumentation Workshop, May 4-7, 1998, SLAC, Palo Alto, CA, USA.

IMPLEMENTATION AND PERFORMANCE OF THE DAΦNE TIMING SYSTEM

G. Di Pirro, A. Drago, A. Gallo, A. Ghigo, F. Sannibale, M. Serio, LNF-INFN, Frascati, Italy

Abstract

In the high luminosity Phi-Factory DAΦNE, a timing system has been provided for the control and proper synchronization of the injection process from the Linac, through an Accumulator/Damping Ring, into the e⁺/e⁻ Main Rings, for the minimization of phase oscillations at injection and for the stability control of the Interaction Point. The Linac beam (e⁺ or e⁻, alternatively) is injected at ≤ 50 pps into an intermediate ring until the required intensity and emittances are reached, then the extraction from the damping ring and injection into a single bucket of the e⁺ or e⁻ ring takes place at ≤ 2 pps. The accumulator RF phase, the firing instant of the Linac, of the injection/extraction kickers in the accumulator ring and of the injection kickers in the main ring must be properly synchronized in order to fill the selected bucket. In this paper we describe the operative procedures and the control programs, along with the hardware solutions and the technologies employed to get the synchronization signals within the required precisions, according to the type of timed element, down to a few picoseconds in the RF chains.

1 INTRODUCTION

DAΦNE is a Phi-Factory [1] with high luminosity at 1020 MeV in the center of mass and large currents distributed in ≤120 bunches. The collider proper consists of two storage rings, one for electrons, the other for positrons, intersecting in two interaction regions. The intense current needed for high luminosity is supplied by a powerful injection system composed of an e⁺/e⁻ Linac [2], a small intermediate storage ring (Accumulator-Damping Ring) [3] and transfer lines ~180 m long.

Injection from the Linac through the Accumulator takes place at the collider operating energy of 510 MeV. The "top-up" injection has been demonstrated during the commissioning.

The injector commissioning started in 1995 with short periods of operation as the major components and services became available. The main rings construction has been completed in July 1997. At the end of 1997 the first collisions have been observed and now the single bunch luminosity commissioning is in progress.

2 DAΦNE REQUIREMENTS

The Linac beam (e⁺ or e⁻, alternatively) is ~10 nsec FWHM long. It is injected in single turn/single bucket at ≤ 50 pps into the Accumulator/Damping Ring (DR) until

the required current is reached. At this point the Linac injection stops and ≥100 msec are left to the stored beam to damp down to the equilibrium dimensions and emittance. The "cooled" beam is then extracted in a single turn and transferred to the main ring (MR), where injection in the desired single bucket takes place at ≤ 2 pps.

The sequence of operations may be different for electrons and positrons. The execution of a required command sequence is performed under control of a timing system. Four resonant discharge coil kickers [4] provide the ~ 200 nsec long injection and extraction pulses in the DR. Different kicker voltages and trigger timing have to be provided between injection and extraction. Similar kickers are used for the injection into either one of the MR's.

It is noteworthy that the e⁺/e⁻ beams to and from the DR pass through portions of the same transfer line in opposite directions, hence the necessity of pulsed magnets [5]. One of these magnets (DHPTT02) is normally off during the DR injection and must be on during the transfer to the MR. In the other pulsed magnet (DHPTT01) the bending field must be reversed between DR and MR injection. The field reversal occurs during the same ~100 msec when the DR beam is being damped. In addition, a third pulsed magnet (DHPTS01) is used to send the Linac beam into a spectrometer branch to measure the mean energy and energy spread. This is done by stealing one Linac pulse onto the spectrometer typically at the same time when the cooled beam is extracted from the DR into the MR.

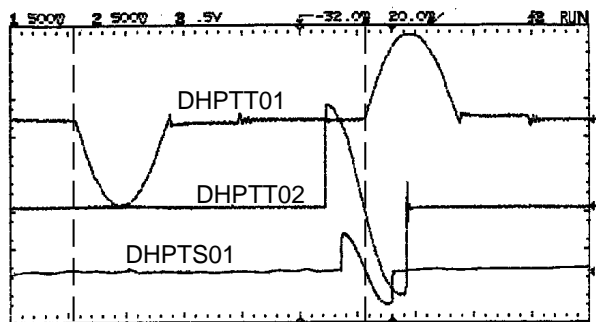


Figure 1 - Pulsed Magnets: dB/dt

In order to fill the selected MR bucket with good efficiency, the firing instant of the Linac modulators and gun, of the injection/extraction kickers in the DR and in the MR, and of the three pulsed magnets must be properly synchronized. The main ring RF drive (368.26 MHz) is provided by a master oscillator; the accumulator RF drive

is derived from the master by digital division and phase shift by the timing system.

The principal parameters of DAΦNE accumulator and main rings relevant to the timing system are presented in Table 1.

Table 1: Rings parameters list

	Main rings	Accumulator
Circumference (m)	97.69	32.57
MR/DR length ratio		3
RF frequency (MHz)	368.26	73.652
Harmonic number	120	8
Number of bunches	1÷120	1
Damping time L/T [msec]	18/36	11/21
Current/bunch (mA)	44	132

The harmonic number ratio between main rings and accumulator is 15 (factor 3 from length ratio, factor 5 from RF frequency ratio). The correct bucket selection in the accumulator is done by proper choice of Linac gun and injection kickers timing. Twenty-four main ring buckets are available for a fixed phase of the accumulator RF. In fact, injection from any of the 8 accumulator buckets into any 1/3 of the main ring is possible by proper delay of the extraction kicker timing. By shifting in phase the accumulator RF by 0 to 4 increments of $2\pi/5$, all 120 buckets in the main ring are available.

3 TIMING SYSTEM OPERATIONAL DESCRIPTION

In this chapter the main operational characteristics of the timing system are presented.

The DAΦNE timing system provides:

- triggers for all the pulsed elements;
- synchronization of the ring RF cavities;
- triggers for the bunch-by-bunch feedbacks;
- triggers for diagnostics and data acquisition system;
- control of operational sequences for all the accelerator.

During the commissioning and the operation many injection sequences have been used, according to the operation mode.

The principal devices to be synchronized and the actions performed by the timing system are listed in Table 2. The combined action of the timed devices is described by a 31 bits "state word" issued by the timing system every 20 msec. One or more state word bits [6] are associated to the specific devices to enable or disable their actions.

The synchronization of the RF cavities of the electron ring and the positron ring is crucial in order to optimize the luminosity. The bunches entering the interaction region coming from the two different rings have to cross in the longitudinal position corresponding to the minimum of the vertical betatron function. The control of the IP is accomplished by means of precision phase shifters inserted between the common master oscillator and the RF cavity drivers.

At the same time the capability of topping-up the main ring requires that the RF phase is the same for the interaction and the injection. Once the MR RF phases are properly set, the accumulator RF phase has to be corrected for the different length of the electron and positron transfer lines. This is done by introducing an offset in the bucket number and a proper delay in the accumulator RF when switching from one particle mode to the other.

Table 2 : Devices to be synchronized

Device	Trigger	Stability	Description
Linac Gun	$\emptyset 4 + (RF/120 + \# \text{ bunch})$	<1nsec	Trigger Linac Gun (~ 10 nsec FWHM)
Linac System	$\emptyset 4 + (RF/120 + \# \text{ bunch})$	<1nsec	Trigger Linac Pulse Modulators
Spectrometer	$\emptyset 2 + (RF/120 + \# \text{ bunch})$	<1nsec	Trigger SEM Hodoscope ADC
Pulsed Magnets	$\emptyset n + (RF/120 + \# \text{ bunch})$	<20μsec	Bending in the Transfer Line
Damping Ring RF	RF/5 + # bunch	<2 psec	Accumulator RF drive
Accumulator Kickers	$\emptyset 4 + (RF/120 + \# \text{ bunch})$	<1nsec	Accumulator inject./extract.
e ⁻ /e ⁺ MR Kickers	$\emptyset 4 + (RF/120 + \# \text{ bunch})$	<1nsec	Inject. into e ⁻ e ⁺ main rings
Injection / Extraction Diagnostics	DR Injection Trigger, MR Injection Trigger	<100ps	Beam Measurements in the DR, in the TL and in MR
Stored Beam Diagnostics	MR Injection, Fiducial	<100ps	MR and IR Beam Measurements
e ⁻ /e ⁺ Long. Feedback	RF, Fiducial	<10psec	Synchronizing Bunch-by-Bunch Feedback
KLOE Experiment	RF/4	<2 psec	Machine Trigger

4 IMPLEMENTATION AND PERFORMANCE

A stable and flexible timing system [7] has been designed and realized to accomplish the DAΦNE requirements.

4.1 *Slow Triggers, fast triggers*

To drive many devices, different triggers have to be generated from the main trigger sources (the 50 Hz and the radiofrequency at 368 MHz). It is possible to synchronize slow triggers (≤ 50 Hz) with fast triggers by circuits based on type D flip-flops. The goal is to have fast triggers as stable and precise as possible respect to the main ring RF and slow triggers also stable but following the fluctuations of the mains. This is to manage better the Linac modulator ripples. The combination between different triggers is possible because the information is basically contained in the phase and not in the frequency.

About the fast triggers, the main ring revolution frequency is obtained dividing the radiofrequency by the harmonic number: to inject in multibunch mode it is necessary to have it with two different phases, one as a fixed reference, the other as a mobile reference according to which bucket the operator wishes to fill. We call "Fiducial" the fixed phase reference, and "RF/n + # bunch" the mobile phase reference; n can be 120 or 5. The Fiducial is mainly used by the diagnostic system, the "RF/n + # bunch" is sent, combined with the convenient slow trigger, to the timed devices in the accelerator plant.

About the slow triggers, the Master Trigger Generator at 50 Hz, through a PLL locked to the mains, generates 4 phases that we call $\emptyset 1$, $\emptyset 2$, $\emptyset 3$, $\emptyset 4$. They are out of phase by exactly 90° . The other slower triggers (25 Hz or less) are created by a software finite state machine based on digital signal processors.

4.2 *Modules*

Several different modules have been designed and implemented at LNF to perform three types of tasks.

A first group of modules creates periodic signals with frequencies derived from the RF master allowing the DAΦNE control system to change their phases in real time. The bulk of the circuits is based on 100E ECLinPS chip family working up to 1 GHz; special care has been used in the design to contain the phase jitter within few picoseconds. This is done by using delay line chips inside the boards and designing printed circuit boards with traces at controlled characteristic impedance.

The most critical part of the timing system consists in creating the signal to drive the damping ring radiofrequency cavity with phases depending on the bucket to be filled; for this signal the rms jitter standard deviation measured in laboratory is 1.4 psec for all the buckets. Besides, two independent Fiducial triggers have been compared for more than a week without showing any bucket skip.

A second group of modules distributes and receives every 20 msec synchronous commands from VME crates to VME crates in all the accelerator area, using a RS485 serial link at 1 Mbit/s. These boards are based on the digital signal processor AT&T DSP1610. The information is contained in the 31 bits state word that is distributed in real time. A local decoder module enables or disables a specific trigger depending on the current state word.

Finally, the last group of modules distributes and adapts signals between different electric levels: pure sinusoidal, differential ECL, NIM, and TTL.

4.3 *Real time finite state machine*

A finite state machine is implemented by the real time software running on the DSP's. Two 50 Hz phases, $\emptyset 1$ and $\emptyset 2$, are used by the module that has to dispatch the timing state words: in this way is possible to manage 4 states correlated with the 50 Hz phases without adding any jitter due to the software. This is important to send synchronized commands. The 4 states are useful to perform all the tasks and to transmit information without putting any device in an unwanted condition.

The command sequences cyclically executed by the finite state machine are files edited in table form. Every table corresponds to a kind of injection. The bunch selection is in another file. This is to maintain the maximum of flexibility with a minimum of files.

Another important feature is the possibility to disable from the main panel a specific trigger for a chosen device, for example to stop the damping ring extraction but not the injection. The timing system can easily do it clearing only the extraction triggers and maintaining enabled the injection ones.

ACKNOWLEDGMENTS

The authors wish to thank U. Frascaco, O. Giacinti, D. Pellegrini, F. Ronci, F. Rubeo for the efforts in realizing the boards. Special thanks to O. Coiro who has also designed the Master Trigger Generator at 50 Hz and to G. Felici for early work in the fast system. Thanks to P. Possanza to have put in final form this paper.

REFERENCES

- [1] C. Biscari and DAΦNE Commissioning Team, "DAΦNE Commissioning", these Proceedings.
- [2] R. Boni et al. "Linac DAΦNE Operational Performance", these Proceedings.
- [3] M.E. Biagini et al., "Performance and Operation of the DAΦNE Accumulator", these Proceedings.
- [4] S. De Simone and A. Ghigo, "DAΦNE Accumulator Kickers", EPAC'92, Berlin, March 1992, p.1449.
- [5] C. Sanelli et al., "The Pulsed Power Converters of the Beam Transfer Lines at DAΦNE / INFN-LNF", these Proceedings.
- [6] G. Di Pirro et al., "The DAΦNE Timing States Update", DAΦNE Technical Note CD-8, INFN-LNF, Accelerator Division, February 25, 1997, Frascati.
- [7] A. Drago et al., "The DAΦNE Timing System", EPAC'96, Sitges, June 1996.

DAΦNE MAGNET POWER SUPPLY SYSTEM

R. Ricci, C. Sanelli, A. Stecchi, LNF-INFN, Frascati, Italy

Abstract

The e^+e^- , 1020 MeV at center of mass, Particle Accelerator Complex DAΦNE, consists of a linear accelerator (Linac), a damping ring (D.A.), nearly 180 m of transfer lines (T.L.) and two storage rings (S.R.), that intersect each other in two points (I.P.), for Φ particle production. The D.A., T.L. and S.R. magnets are powered by means of 462 power supplies, rating from 100 W to 1 MW. The very different output currents, from 10 A to 2300 A, and output voltages, from 8 V to 1300 V, imposed many different technical solution realized by the world industry (Danfysik - Denmark, Hazemeyer - France, Inverpower - Canada, OCEM - Italy). This paper describes the Power Supply System giving also a description of the different typologies, their characteristics and control systems. The paper reports also the power supply performances and gives information on their installation and first year operation period.

1 INTRODUCTION

The Φ -factory DAΦNE [1] is an accelerator complex, shown in Fig. 1, that consists of:

- e^+e^- Linac
- ≈ 180 m of transfer lines
- e^+e^- Accumulator/Damping Ring
- two pseudo-elliptic storage rings

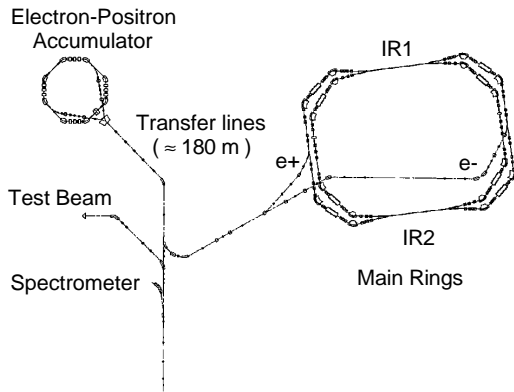


Figure 1: Layout of DAΦNE accelerators and transfer lines.

Electrons and positrons beams are generated and accelerated up to the nominal energy of 510 MeV along the Linac. Then they are transferred, stored and phase space damped in the D.A., with an injection rate of 50 Hz. The beams are then transferred and injected in the S.R. with an injection rate of 1 Hz. The overall injection time should be ≤ 10 minutes, including the time necessary to switch the Linac and the T.L. from positron to electron mode.

The expected S.R. beam life time is ≈ 2 hours.

The Linac, and the related Power Supply System, was assigned on the base of a “turn key” contract and is not described in this paper.

2 THE DAΦNE CONVERTERS

2.1 Transfer Line Converters

The same T.L. is used to transfer the beams from the Linac to the D.A. and from the D.A. to the S.R. This requirement implies that:

- three special magnets have to be powered by pulsed power supplies
- the power supplies powering dc magnets must reverse their current.

The first pulsed converter powers a bending magnet that deflects the incoming beam, from the Linac, toward an energy spectrometer. The second one deflects the beam toward the D.A. during the beam injection and must reverse the magnetic field in the magnet during the damped beam extraction. The third one, normally at zero current during the injection into the D.A., must be switched on during the injection into the S.R. Detailed information on these power supplies may be found in [2].

All the other magnets are powered by means of dc power supplies.

The T.L. have 109 magnets in total that are powered by 140 converters. Table 1 summarizes their characteristics.

Table 1: T.L. Power Supply characteristics

Power Supply for	N.	I_{max} (A)	V_{max} (V)
dc Dipoles	21	100 ÷ 700	25 ÷ 80
Pulsed Dipoles	3	650	1300
Quadrupoles	46	100	25
Injection Septa	8	2300	8 ÷ 50
H/V Steering	62	± 10	± 15

To decrease the number of different power supplies, they have been grouped in 7 types listed in Table 2. The converters for the pulsed magnets are not included in Table 2.

Table 2: T.L. Power Supply Types

Type n.	I_{out} (A)	V_{out} (V)	Power (kW)	N.
1	700	70	49	3
2	280	40	11.2	9
3	120	110	13.2	11
4	100	25	2.5	46
5	2300	8	18.4	4
6	2300	50	115	4
7	± 10	± 15	0.15	62

The specified characteristics are listed below:

Three phase, 50 Hz mains voltage	V 380±10 %
Ambient Temperature	°C 0÷40
Current Setting & Control Range	0÷100 % f.s.
Normal Operating Range	70÷100 % f.s.
Current Setting Resolution	<±1 * 10 ⁻⁴
Current Readout Resolution	<±1 * 10 ⁻⁴
Current Reproducibility	<±5 * 10 ⁻⁴
Residual Current Ripple (peak to peak)	<±1 * 10 ⁻⁴
Long Term Current Stability (8 hours)	<±1 * 10 ⁻⁴

They apply to all the power supplies, except for the H/V Steering power supplies where the Current Setting Resolution, Current Readout Resolution, Residual Current Ripple and Current Stability were relaxed to <±5*10⁻⁴.

2.2 Accumulator/Damping Ring Converters

The D.A. is a dc machine where the Linac beam is first injected at 50 Hz in one RF bucket, damped, extracted at ≈ 1 Hz and injected into a single DAΦNE bucket.

A total of 22 converters, listed in Table 3, power the D.A. magnets. All the dipoles of the ring are series connected, meanwhile the quadrupoles are grouped in three families and the sextupoles in two families. The steering magnets, combining the horizontal and vertical correction, are individually powered.

Table 3: D.A. Power Supply characteristics

Power supply for	N.	I _{out} (A)	V _{out} (V)
Dipoles	1	750	250
Quadrupoles	3	315	80
Sextupoles	2	336	30
H/V steering	8	±10	±15±25

The following characteristics were set more stringent than for T.L. power supplies:

Normal Operating Range	50÷100 % f.s.
Current Setting Resolution	< 5 * 10 ⁻⁵
Current Readout Resolution	< 5 * 10 ⁻⁵
Current Reproducibility	<±5 * 10 ⁻⁵
Residual Current Ripple (peak to peak)	<±5 * 10 ⁻⁵
Long Term Current Stability (8 hours)	<±5 * 10 ⁻⁵

2.3 Storage Ring Converters

In DAΦNE electrons and positrons circulate in two separated storage rings (see Fig. 1) laying in the same horizontal plane with horizontal crossing in 2 * 10 m long interaction regions (IR1 and IR2), at an angle of 25 mrad. These interaction regions will house the experimental detectors KLOE and FINUDA. In DAΦNE the eight bending dipoles and the central poles of the four wiggler magnets of each ring are series connected and powered by means of ≈ 1 MW, 20 kV input voltage, power supplies. All the other magnets are individually powered by dedicated power supplies. Table 4 summarizes the main characteristics of the power supplies of the S.R.

Table 4: S.R. Power Supply characteristics

Power Supply for	N.	I _{max} (A)	V _{max} (A)
Bending Dipoles	2	750	1250
Dipole Back Legs	16	±10	±20
Wiggler Central Poles	2	750	1250
Wiggler End Poles	8	750	120
Quadrupoles	94	585	45
Sextupoles	32	336	25
Splitter magnets	8	750	80
“C” Steerings	16	±215	±25
“Lambertson” Steerings	16	±215	±6
Rectangular and Square Stee.	64	±10	±20
H/V Steerings	32	±215	±10
Skew Quad. Correctors	16	280	40

The other characteristics are the same of the D.A. power supplies, except for the power supplies of the steering and corrector magnets that are the same of the T.L. steering power supplies.

3 TYPOLOGIES

Many different typologies of power supplies have been adopted according to the power supply output current and power rates and to the specific experience of the builder. A list of the typologies, and related company names, of the DAΦNE converters follow.

- SCR’s Graetz Bridge Converter with Active Filtering [HAZEMEYER, OCEM];
- SCR’s Graetz Bridge Converter with Transistor Output Bank [DANFYSIK];
- Diode’s Graetz Bridge Converter with Transistor Output Bank [DANFYSIK];
- Series Double Resonant Switching Converter [OCEM];
- Zero Voltage Switching (ZVS) Converter [DANFYSIK];
- Hard Switching Converter [INVERPOWER];
- Bipolar Linear Converter [DANFYSIK; HAZEMEYER, INVERPOWER];
- Bipolar Switching Converter with 4 Quadrant Output Chopper [INVERPOWER].

The SCR’s Graetz Bridge scheme has been adopted when high output currents were requested as for the S.R. Bending Dipole and Wiggler magnets. In this case two six-phase bridges in series were used. In other cases, e.g. for the high current T.L. dipole magnets and the S.R. Splitter magnets, the two six-phase bridges are in parallel.

The configuration with SCR’s rectifying bridge and Transistor Bank on the output was chosen to power the D.A. dipole and quadrupole magnets, whereas the variant with diode’s rectifying bridge was employed for the D.A. sextupole magnets.

The Series Double Resonant Switching configuration, working between a low resonant frequency of 20 kHz and a high resonant frequency of 100 kHz, was adopted up to 13.2 kW output power and with a maximum of 280 A output current for the air cooled converters of the T.L. dipole and quadrupole magnets. In this typology the current is regulated by varying the switching frequency.

A ZVS full IGBT's bridge configuration, phase modulated, was chosen to power all the multipole magnets of the S.R. The IGBT's switching frequency is fixed at 20 kHz and the output current is controlled by comparing the set current with the one measured by a high precision DCCT. DANFYSIK developed this solution for the first time producing a modular, very compact, water cooled converter. Three converters were located in the same rack.

The Hard switching configuration, with a full IGBT's/MOSFET's bridge, was employed to power the Skew Quadrupole Correctors of the S.R.

Also in this case the converters are water cooled.

The classic Bipolar Linear configuration was chosen for the low current steering magnets of the T.L., D.A. and S.R. Dipole Back Leg correcting windings. The same configuration was developed by DANFYSIK for the "C" and "Lambertson" steering magnets of the S.R.

Finally, the Bipolar Switching Converter with a four quadrant MOSFET's chopper on the output typology was adopted by INVERPOWER for the horizontal and vertical steerings of the S.R.

4 CONTROL SYSTEM

4.1 Abstraction Process

The main issue in developing the computer control was to keep simple and uniform the procedures for the power supplies remote management. Even though all the power supplies have a serial interface (RS422/485) and an internal microcontroller, they follow different protocols. Dealing with several communication standards, it has been necessary to define an abstraction of the power supply object characterized by a set of variables for the readbacks relevant to the control and services for acting on the element itself. The abstraction process allows the user to have information on status and analog readouts always presented in a uniform way and to treat any operation always as a single entity, despite the fact that the operation may actually be achieved by a complex sequence of lower level actions.

4.2 Low Level Control and Tests

The debugging of low level drivers has been carried out during the acceptance tests with a portable computer (Macintosh PowerBook 180c) running LabVIEW® [3] which is the same development environment adopted for the DAΦNE Control System[4]. The use of a high level software tool such as LabVIEW allowed to develop "on the spot" a huge amount of VIs (Virtual Instruments) for

issuing commands and getting information through the power supplies serial interface. Those VIs have been extensively used during the acceptance tests and then embedded, with no significant modifications, into the Command and Control tasks presently running on the distributed CPUs of the DAΦNE Control System.

5 PERFORMANCES

The performances of the converters in general meet the specification, in terms of Current Setting, Control Range, Normal Operating Range, Current Setting and Readout Resolution, and Current Reproducibility. The specified Long Term Current Stability was achieved and in some cases exceeded by all the converters. However, the specification on the Residual Current Ripple caused some problems, mainly on converters of new production. Accurate setting of the active filtering, where foreseen, was a resolute tool. A fine regulation of converters that power multipole magnets, together with a relaxation of the specification by a factor less than two, was necessary but, in any case, it was proved not to be harmful to the circulating beams. Particular attention was dedicated to the EMC compatibility and to the harmonic content of the absorbed primary currents, reducing them to acceptable levels by fine tuning of the rectifying bridges of high power converter and appropriate filtering. In particular, all the switching converters were officially tested according to the German VDE 0875N norms (type tests).

6 FIRST YEAR OF OPERATION

First year of operation pointed out few problems mainly related to random failures of some components (breakers, auxiliary transformers, IGBT's, IC's, etc.) without any serious consequence and promptly repaired in collaboration with the builders.

A major problem, still on the table, concerns some IC's that thermally degrade reducing the threshold between logic levels. This causes the internal control logic to detect an "alarm" state even though the PS is working regularly and drives consequently the converter in Standby mode. This problem is under evaluation and near to be solved.

REFERENCES

- [1] Performances of DAΦNE - This Conference.
- [2] C. Sanelli, S. Vescovi and F. Völker, "The pulsed power converters of the beam transfer lines at DAΦNE" - This Conference.
- [3] LabVIEW® is a trademark of National Instrument Corporation. 6504 Bridge Point Parkway Austin, TX 78730-5039.
- [4] G. Di Pirro, C. Milardi, A. Stecchi and L. Trasatti, "DANTE: control system for DAΦNE based on Macintosh and LabVIEW", Nuclear Instrument and Methods in Physics Research A 352 (1994) 455-457.

INSTALLATION AND ALIGNMENT OF THE DAΦNE ACCELERATORS

C. Biscari, F. Sgemma, LNF-INFN, Frascati, Italy

Abstract

Installation, alignment and survey of the magnetic elements and vacuum chambers of DAΦNE are described. The networks of the Damping Ring and two Main Rings are described, focusing the techniques chosen to obtain the required precisions. A description of the mechanical measurements, coupled to the magnetic ones, to refer the magnetic axis of quadrupoles and sextupoles to their fiducials is underlined: emphasis is put on the strategy to couple precision with quickness. The results of first phase alignment job and its refinement are analyzed using the orbit measurement.

1 INTRODUCTION

DAΦNE (Double Annular Φ-factory for Nice Experiments)¹ is a high luminosity double ring e^+/e^- Φ-Factory with a short term luminosity goal $L=1.3 \cdot 10^{32} \text{cm}^{-2} \text{sec}^{-1}$.

The injector consists of an e^+/e^- Linac and an Accumulator/Damping Ring, connected to DAΦNE through ~ 160 m long Transfer-lines. The machine general layout occupies three areas (see Fig. 1), which were previously occupied by ADONE and have been adapted to the new machine and experiments.

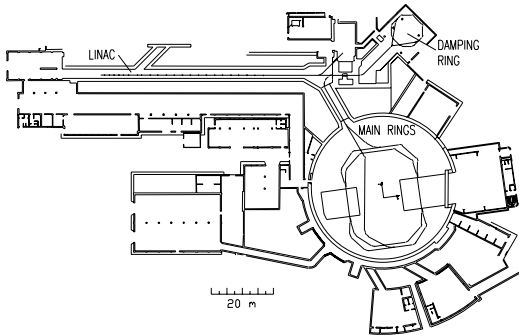


Figure 1: DAΦNE complex layout

The two Rings of the collider are co-planar (see Fig. 2) and each of them, comprised in a rectangle 31 m large and 26 m high, contains 8 bending magnets with a C structure, 4 wigglers, 39 quadrupoles and 16 sextupoles of two different families (“small” and “large”, depending on the internal bore), one rf cavity, 30 corrector magnets. In the Interaction Regions, shared by the two rings, 4 splitter magnets and 4 superconducting solenoids are placed. In the “Day One” configuration, i.e. without experiments, the Interaction Regions contain 14 quadrupoles.

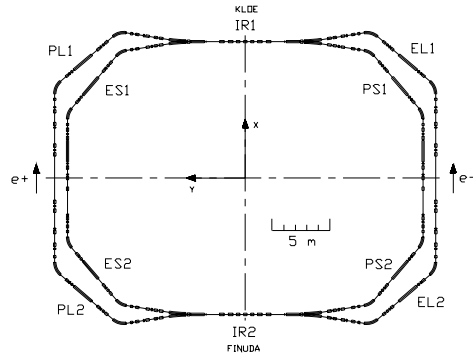


Figure 2: Main rings layout

2 GENERAL NETWORK

A general network, connecting the three separate installation areas, have been defined to allow an alignment with respect to a reference system based on the DAΦNE Main Rings symmetry axis (see Fig. 3). The number of nodes and their position has been defined using the criterion of having at least two nodes in each area and putting them, if possible, along significant lines.

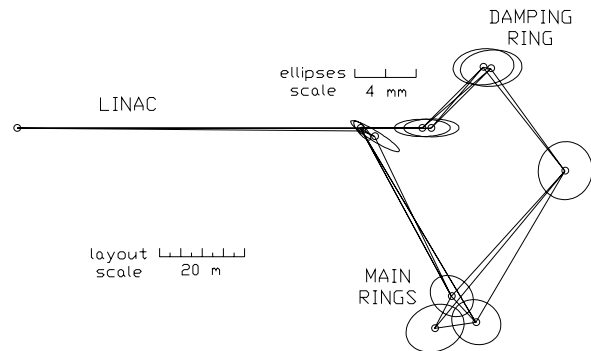


Figure 3: General network

This network has been realized with sockets, with a 30 mm diam. bore and a conical fit for Taylor-Hobson spheres, mounted on pillars or directly inserted in the floor.

A network pre-analysis, which takes into account the number and type of measures (distances and angles) and their precision, allowed to calculate for each node the dimensions of the 99% probability ellipse. This pre-analysis, made with STAR*NET, a Starplus Software Inc. program, showed a maximum ellipse semi-major axis of 1.9 mm.

The survey of the network has been realized measuring angles and distances with the Leica theodolite T3000 equipped with the D2000 Distomat.

3 LOCAL NETWORKS

Two local reference networks were defined and realized: one for the LINAC, based on five nodes in the floor along a line parallel to the LINAC axis at a distance of 1 m, and another one for the Main Rings, made by 15 sockets on pillars. Figure 4 shows the MAIN RINGS local network, together with a schematic layout of the two RINGS, and the 99% probability ellipses.

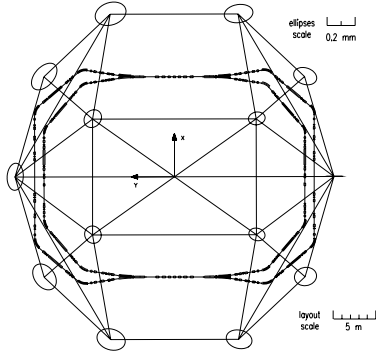


Figure 4: Main ring network

The Main Ring network was designed to have two nodes in each quarter of the machine for distance measurements between them and the bending magnets (8 nodes in total); the other 6 external nodes have been defined to connect the former 8 and to set references to align the experiments. The network pre-analysis showed a maximum ellipse semi-major axis of 0.1 mm. The survey of this network was realized measuring distances with invar wires and the Distinvar instrument, designed at CERN, with a precision of 0.05 mm; the wires were calibrated at CERN. Angle measurements, with a precision of 3", were also performed to increase the redundancy of the network. The socket levels have been accurately measured with Leica N3 Precision Level (± 0.02 mm) with respect to the LINAC axis level (the Damping Ring is 600 mm higher and the Main Ring 500 lower). The levels of many other wall references, realized in LINAC, Damping Ring and Transfer Lines, were measured.

4 DAMPING RING ALIGNMENT

The Damping Ring network, connecting the bending magnets to the local references placed on pillars, is shown in Fig. 5. Only distance measurements, with the invar wires technique, were performed. The pre-analysis maximum ellipse semi-major axis resulted 0.2 mm long. A first rough positioning (± 1 mm) was previously performed, surveying the polar coordinates of bending magnet nodes with theodolite and distomat placed in the center of the machine; a good leveling action was also performed in this phase. Four network surveys, alternated with three adjusting operations between them, were then performed to lower for each node the maximum difference between the measured position and the nominal one to less or equal to 0.1 mm.

After any adjusting action in the horizontal plane a very accurate level adjustment was realized. The bending magnet nodes, when in the final position, were used to align multipoles, correctors, rf cavity, and to survey beam position monitors.

The measured closed orbit with no correction was:

$$x_{rms} = 1.6 \text{ mm}; y_{rms} = 3.7 \text{ mm}$$

From the vertical orbit analysis it was found that it could be corrected by displacing two quadrupoles by -.3, .1mm. After these displacements the residual rms closed orbit is within 1 mm.

The Accumulator runs with no correctors performing above design parameters².

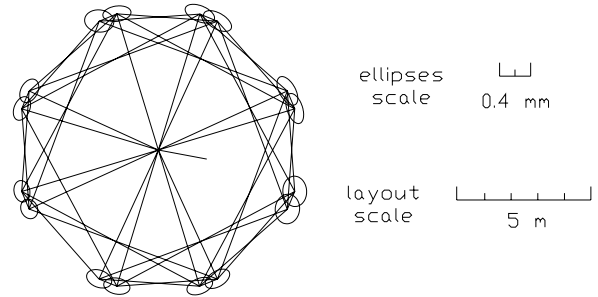


Figure 5: Damping ring network

5 MAIN RING QUADRUPOLES AND SEXTUPOLES MECHANICAL MEASUREMENTS

All the 92 quadrupoles and 32 sextupoles have been magnetically measured with a rotating coil machine, determining the position of the magnetic center with respect to three references on top of each magnet (three 10 mm bores). The orientation of the magnetic axis, passing through the magnetic center, was supposed to be the same of the mechanical axis: for this reason every magnet has been also mechanically measured (see Fig. 6).

To get the three reference bores easily manageable from the survey and alignment point of view, a removable plate was placed on top of each magnet, fitting on tooling balls inserted in the bores: the table bottom surface presents three different features to allow a free but unique, and therefore repeatable, positioning on the magnet. The table is equipped on the top with two micrometer slides on which two Taylor-Hobson sphere sockets are fixed.

The mechanical axis of each magnet has been materialized with a specific tool (a half cylinder, lying on the magnet lower poles, with two marks just along its axis). With the slides in a arbitrary but always equal position, just near the alignment position, seven points have been surveyed for each magnet: the two half cylinder marks, three points on the upper table surface, the two T.H. spheres.

The survey system consists of two theodolites connected to a PC and managed by a LEICA program (ECDS3), able to get 3D coordinates of any point with respect to a reference system based on the theodolites.

The survey process can be separated from the elaboration one: the coordinates of the two T.H. spheres are successively calculated with respect to a reference system with an axis coincident with the magnet mechanical one and another parallel to the table plane. The acquisition process is very accurate (± 0.02 mm) and safe because any discrepancy in collimation between the two operators, one for each theodolite, may be easily detected by the program and verified also later. On the contrary the measuring time has been very short, not more than 20 min/magnet, due in large part to the magnet moving operations and table positioning: the large number of magnets pushed this result.

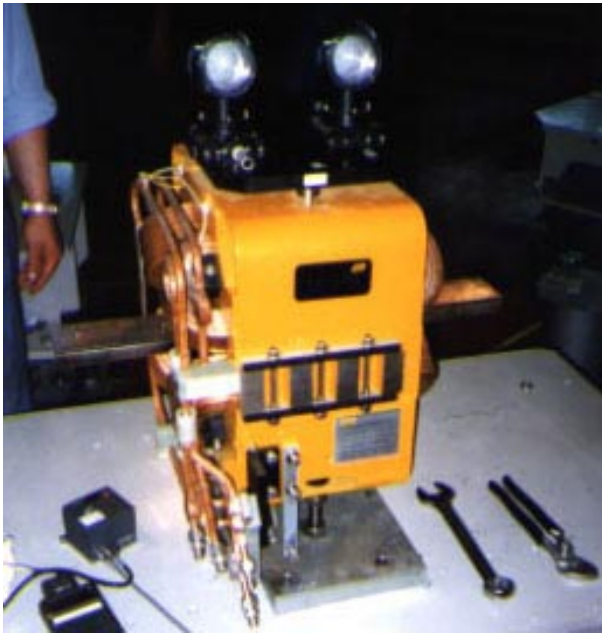


Figure 6: Quadrupole mechanical measurements

As a result of magnetic and mechanical measures we got for any magnet the position of the two slides so that, after the eventual axial rotation, defined as rotation of the table with respect to the horizontal plane, the two T.H. sphere could lie just in the vertical plane passing through the magnetic center and oriented longitudinally as the mechanical axis; with the slides in the specific positions the distances between the T.H. spheres and the plane passing through the magnetic center, oriented as the mechanical axis and perpendicular to the vertical one, were also calculated to complete the information necessary to align the magnet.

6 MAIN RING INSTALLATION AND ALIGNMENT

The Main Ring network, connecting the bending magnets to the 8 local references placed on pillars and between them, is shown in Fig. 7.

Only distance measurements, with the invar wires technique, were performed.

The pre-analysis max ellipse semi-major axis resulted 0.2 mm. Five network surveys and four adjusting operations between them were performed to obtain that for each node the maximum difference between the measured position and the nominal one could be less or equal to 0.1 mm. The bending magnet nodes were used to align and/or survey the other machine components.

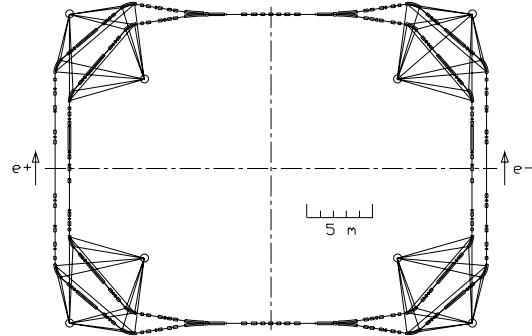


Figure 7: Main Ring Network.

The installation of the bending magnets (C magnets) resulted very critical due to the little clearance (1 mm) between the magnet poles and the arc vacuum chambers, a 10 m long single piece. The arc chambers were installed just after the positioning and rough alignment of magnetic elements involved (with their upper part removed) and then well leveled; at this point the bending magnets, suspended to the crane in a very horizontal way with adjustable cables at the proper height, were slowly horizontally moved to fit the vacuum chamber till around their final position: only then the three legs were lowered to support the magnet weight. Some difficulties for the installation of external bending magnets arose from the little space between the positron and electron machines.

In the first operation of the machine it has been measured that the closed orbit is mainly determined by the "cross-talk" of one ring on the other and by the transfer lines fringing fields on the rings, while the alignment error effect is much smaller. In particular on the e^+ ring displacing three quadrupoles from their nominal positions has been used to correct the vertical bare closed orbit to less than 5 mm. Both rings are stable with no correctors.

7 CONCLUSIONS

All the survey and aligning job has been performed with only two specialized operators, helped by two other not specialized. It must be underlined that the 92 quadrupoles and the 32 sextupoles have been aligned in 25 working days. During the two last years the aligning job has never been a bottle neck for the machine installation and has assured a very good start for the machine commissioning.

REFERENCES

- [1] C. Biscari et al.: "Performances of DAΦNE", these Proceedings.
- [2] M.E. Biagini et al.: "Performance and Operation of the DAΦNE Accumulator", these Proceedings.
- [3] M. Bassetti et al.: "DAΦNE Main Ring Optics", these Proceedings.

THE DAΦNE WATER COOLING SYSTEM

L. Pellegrino, LNF-INFN, Frascati, Italy

Abstract

A water cooling system for the DAΦNE complex has been constructed and operated successfully. Special care has been taken to improve system reliability and temperature accuracy during the design, the realization and the commissioning; specific solutions have been adopted to meet accelerator requirements. Here the design, specifications and results of performance tests are revised.

1 INTRODUCTION

The DAΦNE complex cooling system is divided in three subsystems (LINAC, Damping Ring, Main Rings) and is the heart of the fluid auxiliary system of the whole installation.

More than 1200 meters of piping ranging from 12" to 1" convey treated and cooled water from pumping stations to end users in the accelerator buildings. All pipes are made of stainless steel jointed in situ with high quality TIG welding.

Table 1: DAΦNE complex cooling system data

Cooling Power	9 MW
Users Supply Mean Temperature	32°C
Water (Demineralized)	65000 liters
Water (Towers)	14000 liters
Flow (Demineralized)	133 liters/s
Flow (Towers)	382 liters/s
Tower Makeup Water	4 liters/s
Supply Pressure Range	800-500 kPa
# Towers	6
# Pumps	40
# Distribution Manifolds	147
# Hose Couplings	1780
# Control Loops	26
# Measure Points	384

The cooling system has to fulfill three main requirements: reliability and safety, low level of mechanical vibration and temperature stability and accuracy.

Stable functioning rely on high degree of modularity: each pump or tower has a spare on line, and both work alternatively; moreover each control valve or heater is driven by a stand alone DDC controller put in a network with the main PLC. Therefore a central fault will not affect peripheral units, and greater flexibility is achieved.

Tower water treatment has been employed to minimize makeup and time consuming maintenance operations.

Safety is ensured by automatic section of main branches in case of leakage, high sensitivity flow switch on each distribution manifold, absence of gaskets or sealing due to fittings to prevent leakage for material aging and inert gas tank pressurization to minimize O₂ corrosion. Water conductivity control has been adopted (< 0.5 μS/cm) by on-line mixed bed deionizers and continuous monitoring. Reverse osmosis demineralizer can quickly refill water leakage (e.g. during maintenance work).

In order to reduce vibrations, water velocity in piping has been kept low (less than 1 m/s) and evaporative cooling has been preferred to chillers; as a matter of fact, optical instruments used in surveying magnets (sensitivity 0.02 mm) has shown no appreciable movement.

Here emphasis will be put on preliminary results on temperature control in the Main Rings subsystem.

2 GENERAL DESCRIPTION

The components of Main Rings (magnets, synchrotron light absorbers, power supplies and RF apparatus, divided in three subsystems by pressure level and localization) are cooled by demineralized water. The heat removed is rejected in the secondary side of a rank of heat exchangers. Finally the heat is dissipated in evaporative towers which cool the primary side of the exchangers.

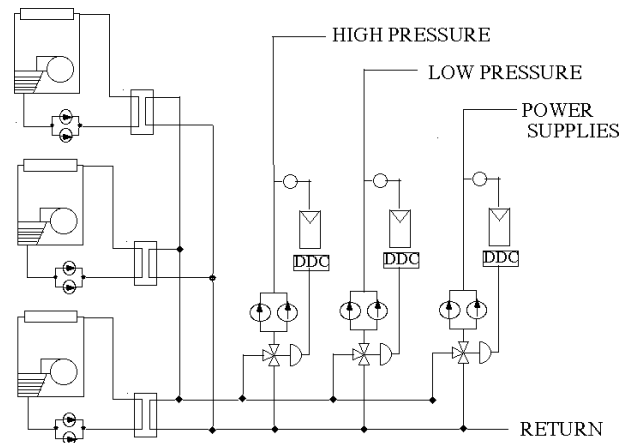


Figure 1: Main rings cooling system schematic

2.1 Temperature regulation system

The temperature regulation is accomplished in three stages: first, cooling towers have a coarse, three steps regulation by progressive fans insertion.

Second, a line of three-way valves on each sub-circuit of the secondary side makes a finer stabilization by mixing fresh and hot (return) water. This stage is sufficient for most accelerator components.

Third and last stage, two kind of different devices arrangements keeps temperature stable up to RF components requirement.

1. A cascade of two electric heaters refines and limits at the lower end the temperature of each RF circulator and coaxial load.

2. Disconnected circuits (sub-sub-systems) for cavities are realized by interposition of a rank of heat exchangers for each cavity. The primary side of these exchangers is cooled by magnet circuit water with a variable flow, three way valve arrangement for first temperature adjustment; at the secondary side, water cools the cavity, keeping temperature under finer control with a cascade of two electric heaters.

A system of pressure driven valves keeps water pressure stable when difference between end users pressure drops could lead to flow disuniformity.

3 MAGNETS SUBSYSTEM WATER TEMPERATURE

3.1 Temperature stability

Thanks to the two stage regulation system, the temperature stability of subsystems is fully satisfactory.

Preliminary data taken in June 1998 at sunset time is shown in Fig. 2. The effect of the two first stages of regulation is clear. The bottom line shows the temperature regulated by the tower fans insertion only; the upper line shows the temperature stabilized by the 3-way valve.

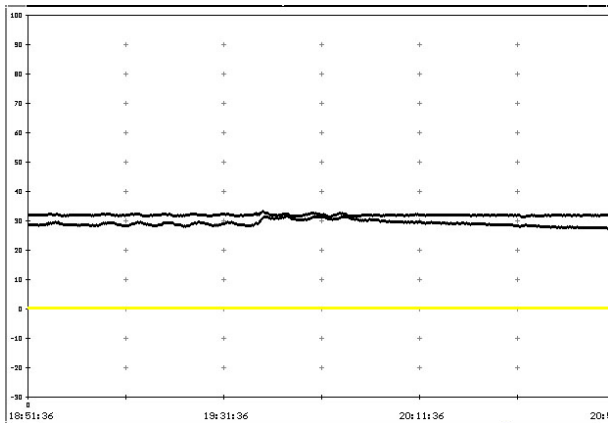


Figure 2: Secondary system temperature stabilization

3.2 Indirect measure of temperature stability

Figure 3 shows the temperature measured on splitter magnets power supply by load resistivity change. The plot obtained is useful an index of the actual temperature stability of cooled coils, taking into account the effect of the thermal capacity of the distribution system and of the magnet itself. The range of temperature is kept very narrow in spite of the large dead time between the control valve and end users.

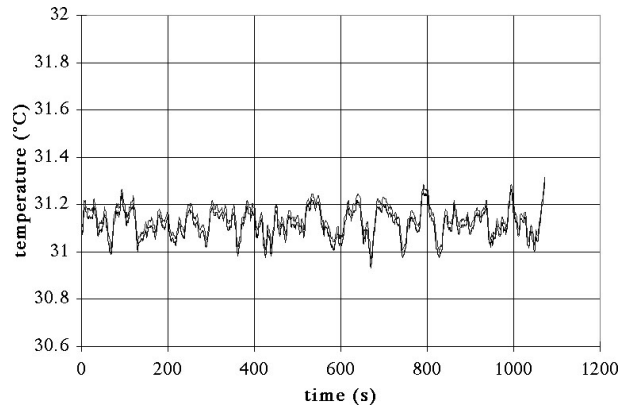


Figure 3: Temperature reading at splitters coils

4 CAVITIES SUB-SUBSYSTEM WATER TEMPERATURE

4.1 Cavity cooling design

The two DAΦNE normal conductive RF cavities are made of copper, with cooling tubes brazed in caves machined on their surface.

The cooling of the cavity body has been designed to keep its temperature uniform within 3°C, to allow homothetic volume changes with coolant temperature (see Tab. 2).

Table 2: Cavity cooling data

Total flow	18	m ³ /h
# of circuits	44	
Tubes inner ø	8	mm
Pressure drop	13	kPa
Water velocity	0.6	m/s

A very accurate 3-D simulation and measurements on the first cavity have been done to verify tubes spacing and coolant flow distribution. The difference in flow among the 44 circuits is below $\pm 8\%$.

A transient analysis has been performed taking into account the actual fluid flow and heat exchange with the body. The results of simulation of the cavity body response vs. time to a step change of the coolant temperature at the inlet of the tubes are shown in Fig. 4.

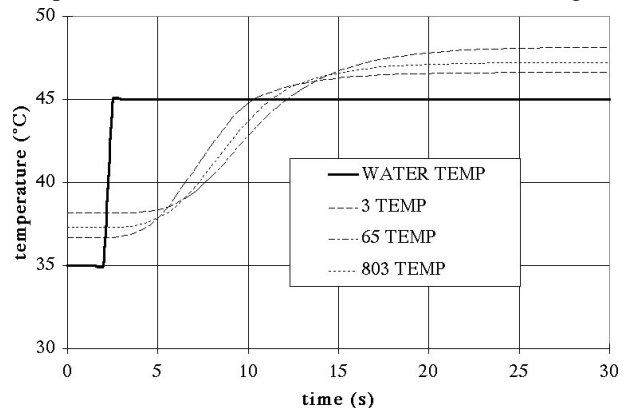


Figure 4: Calculated cavity temperature response

The analysis highlights the really fast thermal reaction of the massive copper body.

Then, thermal-structural analysis has given 0.01-0.02 mm/°C displacements in the range of 35-45°C.

Applying the field distribution calculated in [1], the ensuing resonant frequency shift has been evaluated as 10 kHz/°C in the same range.

4.2 Temperature control loop

The three elements placed in cascade act on the coolant before entering the cavity (see Fig. 5). Two independent loops with the same set point control the 3way valve and the two heaters (50 and 12 kW). The three actions are simultaneous but with different gains and integral effects.

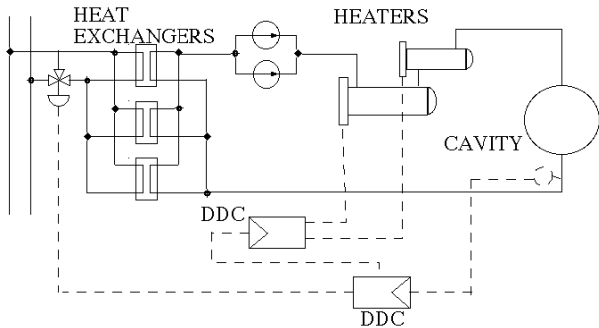


Figure 5: Cavity cooling circuit

4.3 Sensitivity analysis

A first setup of the control loop has allowed a sufficient stable operation of the cavities at fixed temperature (32 ± 0.5°C) during DAΦNE commissioning.

An NI-DAQ board SCXI 1120 and LabView have been employed to remote monitoring four points of the cavity surface during operation.

A data acquisition is reported in Fig. 6, showing the response of the cavity system to a set point step change of 5°C.

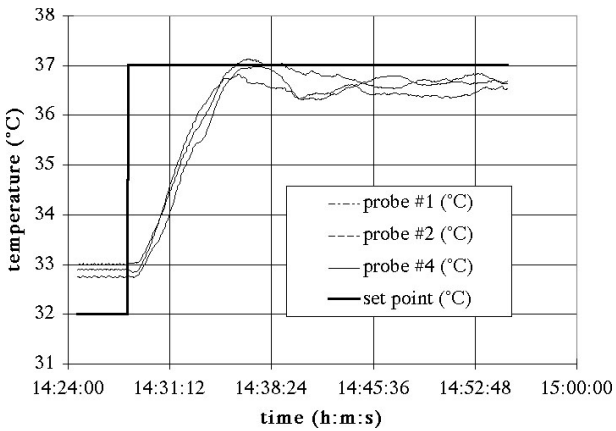


Figure 6: Cavity temperature response to step change

4.4 Cavity response to temperature variation

Recently a check on the effect on cavity geometry and resonant frequency has been performed.

First the tuner position at several temperature set points has been recorded (Table 3, 2nd row). The temperature accuracy available has been enough to ensure stable readings because variations are below the lower limit of the tuner feedback sensitivity.

Then frequency spectra have been recorded with tuner position locked (Figure 7 and Table 3, 3rd row).

Table 3: Effect of temperature variation on RF system

Temperature (°C)	tuner position (mm)	frequency shift (MHz) (tuner off)
32	16.520	368.2326
37	17.071	368.2253
42	17.735	368.1962
47	18.403	368.1668

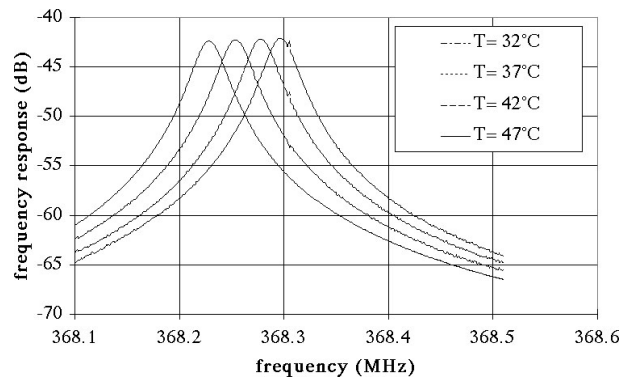


Figure 7: Cavity frequency change with temperature

10 CONCLUSIONS

First operation of cooling system has shown a good adequacy to the required tasks, and permitted successful achievement of DAΦNE Project important milestones.

For cavity circuits, the next goal is to keep the temperature stability within 0.1°C, while having a response to set point changes as fast as possible, should it be needed for RF tuning.

ACKNOWLEDGMENTS

The author wishes to stress the essential role played by the Fluid System Service's Crew during the installation, commissioning and operation of all the systems. Thanks are due to S. Gallo, G. Mazzitelli and G. Di Pirro for their support in RF and splitter magnets data acquisition.

REFERENCES

- [1] P. Arcioni, L. Perregrini, B. Spataro, "Numerical simulations on the DAΦNE RF Cavity", DAΦNE 8th Machine Review, Frascati, Feb. 1995.
- [2] P.A. McIntosh, C.L. Dawson, D.M. Dykes, "Temperature dependent HOM in the SRS cavities", EPAC'96, Sitges, June 1996.
- [3] M. Svandriik, A. Fabris, C. Pasotti, "Simulations and measurement of HOM of the Elettra RF Cavities...", EPAC'96, Sitges, June 1996.